2-

SLAC-PUB-2183
August 1978
(T/E)

WEAK NEUTRAL-CURRENT INTERACTIONS*†

R. Michael Barnett

Stanford Linear Accelerator Center
Stanford University, Stanford, California 94305

I. INTRODUCTION

The structure of gauge theories of the weak and electromagnetic interactions can be studied with the weak neutral-current interactions of quarks and leptons. In gauge theories, the charged currents (CC) are related to the neutral currents (NC). In SU(2) × U(1) models, for example, the determination of the neutral currents follows from the relation (where for simplicity right-handed charged currents are ignored):

$$J_\mu^{NC} = \bar{q}\, C^0 \gamma_\mu (1 + \gamma_5)\, q - 2 \sin^2 \theta_W J_\mu^{em} \qquad (1.1)$$

where q is the vector (u, c, d, s, ...) and J_μ^{em} is the electromagnetic current. C^0 is a matrix obtained from

$$C^0 = \left[C, C^\dagger\right] \qquad (1.2)$$

where C is a matrix giving the appropriate charged current of a given SU(2) × U(1) model, i.e.,

$$J_\mu^{CC} = \bar{q}\, C \gamma_\mu (1 + \gamma_5)\, q. \qquad (1.3)$$

Thus information about neutral currents can determine the existence or non-existence of charged currents such as $\bar{u}b_R$, $\bar{t}d_R$ or $\bar{E}^0 e_R$ where m_t, m_b and m_{E^0} can be arbitrarily large.

*Research supported in part by the Department of Energy.

†Invited talk at the Summer Institute on Particle Physics, Weak Interactions - Present and Future, Stanford Linear Accelerator Center, Stanford, California, July 10-21, 1978.

With the data now available, it is possible to establish uniquely the values of the neutral-current couplings of u and d quarks. The roles of each type of experiment in the determination of these couplings are analyzed in Section II. The section concludes with a discussion of the implications of these results for gauge models of the weak and electromagnetic interactions. Section III contains an analysis of the neutral-current couplings of electrons. The first part of this section presents an analysis of the data based on the assumption that only one Z^0 boson exists. The second part discusses a model-independent analysis of parity-violation experiments. The conclusions are given in Section IV.

II. DETERMINATION OF QUARK COUPLINGS

A model-independent analysis[1] of neutrino scattering data has shown that the neutral-current couplings of u and d quarks could be uniquely determined. The input involved four types of experiments which will be discussed separately. The work[1] described here was done together with Larry Abbott.

It is assumed here that there are only V and A currents. The currents of s and c quarks are neglected. The notation used in this section has u_L, d_L, u_R and d_R (L ≡ left and R ≡ right) as the coefficients in the effective neutral-current coupling:

$$\mathcal{L} = \frac{G}{\sqrt{2}}\, \bar{\nu}\gamma_\mu(1+\gamma_5)\nu\Big[u_L\, \bar{u}\gamma_\mu(1+\gamma_5)u + u_R\, \bar{u}\gamma_\mu(1-\gamma_5)u + d_L\, \bar{d}\gamma_\mu(1+\gamma_5)d + d_R\, \bar{d}\gamma_\mu(1-\gamma_5)d\Big] \qquad (2.1)$$

In the Weinberg-Salam (WS) model[2] with the Glashow-Iliopoulos-Maiani (GIM) mechanism[3] incorporated, u_L is equal to $\frac{1}{2} - \frac{2}{3}\sin^2\theta_W$ with θ_W a free parameter of the theory; u_R, d_L and d_R have similar forms.

Note that there is no assumption about the bosons carrying the neutral current, only an assumption that the effective Lagrangian (2.1) holds.

A. Neutrino-Nucleon Inclusive Scattering

The calculation of deep-inelastic neutrino scattering off nucleons ($\nu N \to \nu X$) is done using the parton model. For sake of discussion only, let us neglect sea contributions and scaling violations (from QCD). For an isoscalar target, one finds that the neutral-current (NC) and charged-current (CC) cross sections for neutrinos are:

$$\sigma_\nu^{NC} = \frac{G^2 mE}{\pi} \int dx\ F(x)\ \left[\left(u_L^2 + d_L^2\right) + \frac{1}{3}\left(u_R^2 + d_R^2\right)\right] \tag{2.2}$$

$$\sigma_\nu^{CC} = \frac{G^2 mE}{\pi} \int dx\ F(x)\ [1] \tag{2.3}$$

Then the ratios for neutrinos and for antineutrinos are

$$R_\nu \equiv \frac{\sigma^{NC}}{\sigma^{CC}} = \frac{\left(u_L^2 + d_L^2\right) + \frac{1}{3}\left(u_R^2 + d_R^2\right)}{(1)} \tag{2.4}$$

$$R_{\bar\nu} \equiv \frac{\sigma^{NC}}{\sigma^{CC}} = \frac{\frac{1}{3}\left(u_L^2 + d_L^2\right) + \left(u_R^2 + d_R^2\right)}{\left(\frac{1}{3}\right)} \tag{2.5}$$

Therefore, one can determine the values of $\left(u_L^2 + d_L^2\right)$ and of $\left(u_R^2 + d_R^2\right)$, which are the radii in the left (L) and right (R) coupling planes. The available data[4] are shown in Fig. 1 along with the predictions of the WS model.

Using the data[4] of the CERN-Dortmund-Heidelberg-Saclay (CDHS) group ($R_\nu = 0.295 \pm 0.01$ and $R_{\bar\nu} = 0.34 \pm 0.03$), the values of the radii in the L and R planes allowed at the 90% confidence level are shown in Fig. 2.

An overall sign ambiguity among the four couplings is resolved by requiring $u_L > 0$.

B. Inclusive Production of Pions by Neutrinos

The allowed radii are well determined by deep-inelastic scattering. It remains to determine the allowed angles in the left and right planes. Let us define

$$\theta_L \equiv \arctan\ (u_L/d_L) \qquad \theta_R \equiv \arctan\ (u_R/d_R) \tag{2.6}$$

One means of determining the angles is through use of inclusive pion production ($\nu N \to \pi X$). Again parton model assumptions are involved in the calculations. This analysis has been discussed by Sehgal, Hung and Scharbach.[5] It is assumed that pions produced in the current-fragmentation region (leading pions) are decay products of the struck quark. If z is defined as E_π/E_{had} (where E_{had} = [total hadron energy] = energy of the struck quark), then $D_q^\pi(z)$ describes the probability that a given pion has a fraction z of energy of the struck quark q. The calculations are similar to those for inclusive deep-inelastic scattering except that the limited specification of the final state requires that the u couplings be multiplied by $D_u^\pi(z)$ and d couplings by $D_d^\pi(z)$. Then the ratio of π^+ to π^- production for neutrinos is (neglecting sea contributions for discussion only):

$$\frac{N_{\pi^+}}{N_{\pi^-}} = \frac{\left(u_L^2 + \frac{1}{3}u_R^2\right)F_u^{\pi^+} + \left(d_L^2 + \frac{1}{3}d_R^2\right)F_d^{\pi^+}}{\left(u_L^2 + \frac{1}{3}u_R^2\right)F_u^{\pi^-} + \left(d_L^2 + \frac{1}{3}d_R^2\right)F_d^{\pi^-}} \tag{2.7a}$$

with

$$F_q^{\pi} \equiv \int_{z_1}^{z_2} dz\, D_q^{\pi} \tag{2.7b}$$

where one requires $z > z_1$ (leading pions), $z < z_2$ (avoids resonance region) and $E_{had} > E_0$; the values of z_1, z_2, and E_0 depend on the particular experiment.

There are isospin relations

$$D_u^{\pi^+} = D_d^{\pi^-} \qquad \text{and} \qquad D_u^{\pi^-} = D_d^{\pi^+} \tag{2.8}$$

which help simplify Eq. (2.7). Furthermore, the ratio of $D_u^{\pi^+}$ to $D_u^{\pi^-}$ can be measured in ep scattering and in charged-current neutrino scattering; the relevant ratio is

$$\eta \equiv \int_{z_1}^{z_2} dz\, D_u^{\pi^+}(z) \Bigg/ \int_{z_1}^{z_2} dz\, D_u^{\pi^-}(z) \tag{2.9}$$

Using Eq. (2.8) and (2.9) in Eq. 2.7, one obtains

$$\left(\frac{N_{\pi^+}}{N_{\pi^-}}\right)_{\nu} = \frac{\left(u_L^2 + \frac{1}{3}u_R^2\right)\eta + \left(d_L^2 + \frac{1}{3}d_R^2\right)}{\left(u_L^2 + \frac{1}{3}u_R^2\right) + \left(d_L^2 + \frac{1}{3}d_R^2\right)\eta} \tag{2.10}$$

For antineutrinos, Eq. (2.10) holds if one interchanges L and R. There are corrections to Eq. (2.10) from sea contributions and from experimental efficiencies.

The data used here are low energy data from Gargamelle[6] at the CERN PS. These data are $\left(N_{\pi^+}/N_{\pi^-}\right)_{\nu} = 0.77 \pm 0.14$ and $\left(N_{\pi^+}/N_{\pi^-}\right)_{\bar{\nu}} = 1.64 \pm 0.36$ for $0.3 < z < 0.7$ and $E_{had} > 1$ GeV. These are shown in Fig. 3

along with the predictions of the WS model.

Recently, high energy data have become available. The neutrino data[6] are not for pions but for all charged particles (within the prescribed cuts); Abbott and I have used electroproduction data to estimate K and p contamination in the signal and find that the results are consistent with the Gargamelle results. The preliminary antineutrino data[6] are also consistent with the low energy data.

We find that the high energy data do not change our conclusions or the final values of the neutral-current couplings obtained from our analysis. However, the error bars would be increased; this is due in part to the fact that the actual quantity used (see Eq. B3 and B4 in the second paper of Ref. 1) involves differences between numbers of the same magnitude.

As can be seen in Fig. 2, the Gargamelle pion-inclusive data (even with 90% confidence levels) place severe restrictions on the allowed angles. However, since the ratios (Eq. 2.10) are functions of the squares of the couplings, there are various sign ambiguities.

C. Elastic Neutrino-Proton Scattering

Further determination of the allowed angles along with resolution of some sign ambiguities can be obtained from analysis[1,7] of elastic neutrino-proton scattering ($\nu p \to \nu p$). Unlike the calculations of Sections IIA and B, no parton model assumptions are needed here. The matrix element for the process is

$$\langle p'|J_\mu|p\rangle = \bar{u}(p')\left[\gamma_\mu F_1 + \frac{i\sigma_{\mu\nu} q^\nu}{2m} F_2 + \gamma_5\gamma_\mu F_A\right]u(p) \qquad (2.11)$$

The vector form factors $\left[F_1(q^2) \text{ and } F_2(q^2)\right]$ are related via CVC to the electromagnetic form-factors of protons and neutrons:

$$\text{Isovector} \quad F_i = F_i^p - F_i^n \tag{2.12}$$

$$\text{Isoscalar} \quad F_i = F_i^p + F_i^n \tag{2.13}$$

The isovector part of the axial-vector form-factor has been measured and has the form:

$$F_A(q^2) = \frac{1.23}{(1 + Q^2/m_A^2)^2} \tag{2.14}$$

where $m_A^2 \simeq 0.79\ \mathrm{GeV}^2$ (our results are not very sensitive to variation of m_A). The isoscalar part of the axial-vector form factor is assumed to have the same Q^2 dependence.

The appropriate factors between these four terms are obtained using the SU(6) wavefunctions of nucleons. The data of the Harvard-Pennsylvania-Wisconsin (HPW) group[8] are $R_\nu \equiv \sigma^{NC}/\sigma^{CC} = 0.11 \pm 0.02$ and $R_{\bar{\nu}} = 0.19 \pm 0.05$ (statistical errors shown). These are shown in Fig. 4 along with the predictions of the WS model.

The resolution of the sign ambiguities remaining from the pion-inclusive data is difficult to see in Fig. 2, since correlations between the left and right planes are not evident. From the pion-inclusive data shown in Fig. 2, one might think that there are 2, 3, or 4 allowed regions. The correlations can be made evident by plotting θ_L vs θ_R (see Eq. 2.6) as in Fig. 5; this can be done "uniquely," because the radii in the left and right planes are well determined. The pion-inclusive data result in four allowed regions (appearing as ellipses in Fig. 5); there would be eight regions except that $d_R \approx 0$ so that four pairs of regions coalesce.

By "inverting" the νp elastic scattering data (with the analysis described above), one can rule out two of these four regions completely and can rule out substantial portions of one other. Varying portions of two regions do remain allowed. Independent of the pion-inclusive data, the elastic data severely limit the allowed regions in coupling space.

D. Production of Exclusive Pion Modes by Neutrinos

Two of the three remaining allowed regions in Fig. 5 can be ruled out by consideration of the cross-section ratios for six exclusive channels containing a pion:

$$\sigma(\nu p \to \nu p\pi^0)/\sigma_1 \tag{2.15}$$

$$\sigma(\nu n \to \nu n\pi^0)/\sigma_1 \tag{2.16}$$

$$\sigma(\nu n \to \nu p\pi^-)/\sigma_1 \tag{2.17}$$

$$\sigma(\nu p \to \nu n\pi^+)/\sigma_1 \tag{2.18}$$

$$\left[\sigma(\bar{\nu}p \to \bar{\nu}p\pi^0) + \sigma(\bar{\nu}n \to \bar{\nu}n\pi^0)\right]/\sigma_2 \tag{2.19}$$

$$\sigma(\bar{\nu}n \to \bar{\nu}p\pi^-)/\sigma_2 \ . \tag{2.20}$$

with

$$\sigma_1 \equiv \sigma(\nu n \to \mu^- p\pi^0) \tag{2.21}$$

$$\sigma_2 \equiv \sigma(\bar{\nu}p \to \mu^+ n\pi^0) \tag{2.22}$$

where recent Gargamelle data[9] were used.

To analyze the data, the detailed pion-production model developed by Adler[10] was used. This model is superior to all other pion-production models; it includes non-resonant production (an important feature), incorporates excitation of the Δ(1232) resonance, and satisfies current algebra constraints. The model gives quite good descriptions of a variety of data and is crucial for analysis of the Gargamelle data.

One begins with the Born amplitudes shown in Fig. 6 which are given in terms of the form factors F_1, F_2 and F_A (described in Section IIIC), F_π (coming from Fig. 6c) and g_r (the pion-nucleon coupling). There are two types of corrections applied.

One comes from using the current algebra relation:

$$T\left\{\partial^\mu J_\mu^5 \mathcal{J}\right\} = -\delta\,(x_0)\left[J_0^5,\mathcal{J}\right] + \partial^\mu\, T\left\{J_\mu^5 \mathcal{J}\right\} \qquad (2.23)$$

(where T indicates time-ordered product, and $\mathcal{J}$ is the weak current of interest). Taking the Fourier transforms and then the matrix element between nucleon states for each piece of Eq. (2.23, one finds from PCAC that the left side is proportional to the desired matrix element $\langle N\pi|\,\mathcal{J}\,(0)\,|N\rangle$. The first term on the right side leads to additional form factor terms. The second term containing the J^5 current with axial-vector couplings, rather than the pseudo-scalar coupling assumed for the pion, implies certain vertex corrections.

The second type of correction is for final-state interactions; the outgoing pion and nucleon can resonate. In particular, for the appropriate $I = \frac{3}{2}$ terms, one must account for the $\Delta(1232)$ resonance. There are the usual phase shifts ($e^{i\delta_R}$) and enhancement effects for this P_{33} resonance. It is <u>crucial</u> to keep the non-resonant (including $I = \frac{1}{2}$) pieces; both the analysis and the data say those pieces are significant.

To avoid other (higher mass) resonances and for consistency with the soft-pion assumptions of current algebra, it is necessary to require that the invariant mass W of the pion-nucleon system be less than 1.4 GeV. Unfortunately, the data are not available with this cut, and for modes with final-state neutrons it is, of course, quite difficult to obtain the invariant mass. However, the relevance of the cut to our conclusions is minimized because: (1) most data are below the W = 1.4 GeV cut; (2) ratios of cross sections are used; (3) application of the cut to the limited experimental mass plots available indicates a strengthening of our conclusions; and (4) the model predictions are assumed to be valid only to within 30% and the data to the 90% confidence level (this is somewhat different from the procedure followed in the first paper of Ref. 1). This fourth point is approximately equivalent to allowing any theoretical values which lie within a factor of two of the various data.

Our analysis of the six exclusive pion-production channels shows that small values of $\theta_L (\theta_L < 90^\circ)$ are totally forbidden by these data. Recall that there were four regions in Fig. 5 allowed by pion-inclusive data, and that two were ruled out by the elastic data. A third region (with $\theta_L \approx 40^\circ$ and $\theta_R \approx 270^\circ$ in Fig. 5) is now completely ruled out. The region with $\theta_L \approx 140^\circ$ and $\theta_R \approx 90^\circ$, which was forbidden by elastic data, is not allowed by these data either. The exclusion of this latter region by these data alone would be much more marginal than for the regions with $\theta_L \approx 40^\circ$. What remains is a single region (with $\theta_L \approx 140^\circ$ and $\theta_R \approx 270^\circ$) which is in good agreement with all four types of neutrino experiments. This unique determination can be expressed in terms of the coupling constants so that the allowed region (see Fig. 2) is

$$\begin{aligned} u_L &= 0.35 \pm 0.07 \qquad & u_R &= -0.19 \pm 0.06 \\ d_L &= -0.40 \pm 0.07 \qquad & d_R &= 0.0 \pm 0.11 \end{aligned} \tag{2.24}$$

where the errors are 90% confidence levels and an overall sign convention $(u_L \geq 0)$ has been assumed.

E. Implications for Gauge Models

In examining the structure of gauge models of weak and electromagnetic interactions, one of the important questions is whether, in the context of SU(2) × U(1) models, there is any evidence for right-handed charged currents. The neutral-current results are directly relevant to this question and indicate that there are no right-handed charged currents for u or d quarks in SU(2) × U(1) models.

This conclusion can be obtained by consideration of Fig. 7 which shows the allowed regions from Fig. 2. All SU(2) × U(1) models with the left-handed coupling doublet $\bar{u}d_L$ have values in the left-coupling plane (Fig. 7a) which are indicated by the line with tick marks. These models have $\sin^2\theta_W$ as a free parameter so that the position on the line (i.e., the value of $\sin^2\theta_W$) is determined solely from the data. Clearly from Fig. 7a, the allowed value of $\sin^2\theta_W$ is between 0.2 and 0.3.

Now looking at the right coupling plane, Fig. 7b, one sees that for the WS model the values of $\sin^2\theta_W = 0.2 - 0.3$ are also allowed there. The overall magnitude of these neutral-current couplings was dependent on the mass ratio of $m(Z^0)/m(W^\pm)$ which is predicted by the WS model[2] with the minimal Higgs boson structure (one or more doublets) to be:

$$m_{Z^0} = m_{W^\pm}/\cos\theta_W \qquad (2.25)$$

If this mass ratio were not as predicted, then the model would be ruled out (for example, one might find that $\sin^2\theta_W = 0.1$ was required by the left-coupling plane, Fig. 7a, but $\sin^2\theta_W = 0.4$ by the right-coupling plane, Fig. 7b). The success of these predictions of the WS model is remarkable.

For other SU(2) × U(1) models, if one chooses $\sin^2\theta_W = 0.3$ from the left-coupling plane, then the resulting points in the right plane are determined. Shown in Fig. 7b are the points for the cases where the models have the right-handed doublets $\bar{u}b_R$ (labeled A),[11] $\bar{t}d_R$ (B)[12], and both $\bar{u}b_R$ and $\bar{t}d_R$ (C). The latter model (C)[13] has been called the "vector" model. As can be seen, these models are ruled out by the data. Varying the ratio $m(Z^o)/m(W^\pm)$ moves the points toward or away from the origin, but these models still cannot survive. There are other SU(2) × U(1) models[14] involving $-\frac{4}{3}$ and 5/3 charged quarks, and these are also ruled out.

The applicability of these results is <u>not</u> limited to SU(2) × U(1) models. For example, there are two SU(3) × U(1) models which are ruled out by these data. One[15] (labeled D in Fig. 7b) has the u quark in a right-handed singlet and the other[16] (E) has the u quark in a right-handed triplet (for this latter case the parameters of the model were chosen to place u_L and d_L in the allowed region in Fig. 7a).

These results also apply to the $SU(2)_L \times SU(2)_R \times U(1)$ model.[17] Since that model can be chosen to have the same values of u_L, d_L, u_R and d_R as the WS model, it is allowed by the analysis of quark couplings. In fact, Georgi and Weinberg[18] have generalized this conclusion by showing that at zero-momentum transfer, the neutral-current interactions of neutrinos in an SU(2) × G × U(1) gauge theory are the same as in the corresponding SU(2) × U(1) theory if neutrinos are neutral under G.

III. DETERMINATION OF ELECTRON COUPLING

A. Analysis of Neutrino and Parity Violation Experiments

There are two types of experiments which are used to obtain information about the weak neutral-current coupling of the electron. The first is neutrino-electron scattering which can be analyzed in a model-independent fashion as was done for quarks. The second involves searches for parity-violation in electron-nucleon interactions. This analysis requires use of the uniquely determined quark couplings obtained in Section II. However, if the results from analysis of parity-violation experiments are to be compared with those from νe scattering (i.e., if g_A and g_V are to be calculated), then one must make the assumption that there is only one Z^0 boson which can carry the relevant weak neutral currents.

One type of experiment involves the search for parity-violation in atomic transitions in bismuth. The details of these experiments have been given elsewhere.[19] Clearly such effects are proportional to the VA interference terms, and, in the case of bismuth, the $(V_{hadron}\ A_{electron})$ term is completely dominant. The optical rotation ρ which is measured is then proportional to this term, i.e., $\rho = KQ_W$, where K is a constant and (with the one Z^0 assumption)

$$Q_W = -4\ V_{had}\ g_A \tag{3.1}$$

If one defines e_L and e_R as the coefficients in the effective neutral-current coupling:

$$\mathcal{L} \propto \frac{G}{\sqrt{2}}\left[e_L\ \bar{e}\ \gamma_\mu(1+\gamma_5)\ e + e_R\ \bar{e}\ \gamma_\mu(1-\gamma_5)e\right] \tag{3.2}$$

then

$$g_A \equiv (e_L - e_R)$$
$$g_V \equiv (e_L + e_R) \tag{3.3}$$

and

$$V_{had} = (2u_L + d_L + 2u_R + d_R)Z$$
$$+ (u_L + 2d_L + u_R + 2d_R)N \tag{3.4}$$

where Z and N are the numbers of protons and neutrons (for bismuth, $Z = 83$ and $N = 126$).

Although there is some question[20] about the atomic and nuclear calculations of K (where $\rho = KQ_w$), present theoretical estimates for K are such that the optical rotations ρ for the two transitions that have been measured are

$$\rho \approx 1.1 \times 10^{-9}\ Q_w \text{ radians} \quad (\text{for } 8757\ \text{Å}) \tag{3.5}$$

$$\rho \approx 1.5 \times 10^{-9}\ Q_w \text{ radians} \quad (\text{for } 6476\ \text{Å}) \tag{3.6}$$

Two experiments report results consistent with zero: the Washington group[20] reports $\rho = (-0.5 \pm 1.7) \times 10^{-8}$ for the 8757 Å transition while the Oxford group[21] reports $\rho = (+2.7 \pm 4.7) \times 10^{-8}$ for the 6476 Å transition. By contrast, the Novosibirsk experiment[22] found $\rho = (-21 \pm 6) \times 10^{-8}$ for the 6476 Å transition.

Assuming that there exists only one Z^0 boson, then the quark couplings (Eq. 2.24) imply that $g_A \approx 0 \pm 0.06$ for the first two experiments, and $g_A \approx -0.4 \pm 0.17$ for the Novosibirsk experiment.

The other type of experiment for which results have been reported[23] involves νe elastic scattering (with $\nu_\mu e$, $\bar{\nu}_\mu e$ and $\bar{\nu}_e e$ measured by various groups). The cross sections for $\nu_\mu e$ and $\bar{\nu}_\mu e$ scattering are (no Z^0 assumption is involved here):

$$\frac{d\sigma^{\nu,\bar{\nu}}}{dE_e} = \frac{G\, m_e}{2\pi}\left[\left(g_V \pm g_A\right)^2 + \left(g_V \mp g_A\right)^2\left(1 - \frac{E_e}{E_\nu}\right)^2 + \left(g_A^2 - g_V^2\right)\frac{m_e E_e}{E_\nu^2}\right] \tag{3.7}$$

where bottom signs are for antineutrinos. For $\bar{\nu}_e e$ elastic scattering, there is an annihilation term (through a W^- boson), so that in Eq. (3.7) $g_V \to g_V + 1$ and $g_A \to g_A + 1$. Knowledge of these cross sections leads to allowed regions in a g_A-g_V plot which are ellipsoidal annuli.

Results have been reported for a SLAC experiment[24] involving the deep-inelastic scattering of polarized electrons off deuterium and hydrogen targets. In this experiment one measures the asymmetry between the cross sections σ_p and σ_a with electrons polarized parallel and antiparallel to the beam. If there are weak parity-violating effects, the asymmetry will be non-zero. The asymmetry is sensitive to both the $V_{had}\,A_{elec}$ and $A_{had}\,V_{elec}$ terms, and furthermore involves no difficult atomic or nuclear calculations.

For an isoscalar target (deuterium) the asymmetry (see Ref. 25) is, with the one Z^0 assumption:

$$\frac{d\sigma_p - d\sigma_a}{d\sigma_p + d\sigma_p} = 64 \times 10^{-5}\, Q^2 \left\{ \left[\frac{2}{3}(u_L + u_R) - \frac{1}{3}(d_L + d_R)\right] g_A + \left[\frac{1 - (1-y)^2}{1 + (1-y)^2}\right]\left[\frac{2}{3}(u_L - u_R) - \frac{1}{3}(d_L - d_R)\right] g_V \right\} \tag{3.8}$$

The SLAC experiment on the inelastic scattering of polarized electrons from deuterium has reported an asymmetry of $(-9.5 \pm 1.6) \times 10^{-5}\, Q^2$ where Q^2 is about 1.6 GeV^2 and $y = 0.21$. This is shown in Fig. 8 along with the predictions of the WS model and the "hybrid" model (described later). Similar results were obtained with hydrogen. A run at a higher value of y may be made in the future.

D. Model Independent Analysis of Parity Violation Experiments

Bjorken[26] has shown how to analyze parity violation experiments in a model-independent fashion (in particular, there is no need to assume that there is only one Z^0 boson). One defines the parity-violation parameters $\epsilon_{VA}^{e,q}$ and $\epsilon_{AV}^{e,q}$ as the coefficients in the effective Lagrangian

$$\mathcal{L} = \frac{G}{\sqrt{2}}\Big[\bar{e}\gamma^{\mu} e \left\{\epsilon_{VA}^{e,u}\, \bar{u}\gamma_{\mu}\gamma_5\, u + \epsilon_{VA}^{e,d}\, \bar{d}\gamma_{\mu}\, \gamma_5\, d\right\} + \bar{e}\gamma^{\mu}\, \gamma_5\, e \left\{\epsilon_{AV}^{e,u}\, \bar{u}\gamma_{\mu}\, u + \epsilon_{AV}^{e,d}\, \bar{d}\gamma_{\mu}\, d\right\}\Big] \tag{3.9}$$

It turns out that more information can be obtained about $\epsilon_{AV}^{e,q}$ than about $\epsilon_{VA}^{e,q}$ from present data. The implications of the results of the Novosibirsk, Oxford and Washington experiments[20-22] in bismuth and of a "hypothetical" $y = 0$ polarized-electron deuterium experiment are shown in Fig. 9, along with the predictions of the WS model.

C. Implications for Gauge Models

The WS model predicts $g_A = -0.5$ (independent of $\sin^2\theta_W$) which is not consistent with the results of the Oxford and Washington experiments, but it is consistent with the results of the Novosibirsk experiment. There is an $SU(2) \times U(1)$ model which predicts $g_A \simeq 0$. This model, called the "hybrid" model, is identical to the WS model except that in addition to the coupling $(\bar{\nu}e)_L$ there is a right-handed coupling $(\bar{E^0}\, e)_R$. However, Marciano and Sanda[27] have shown that higher order corrections in the hybrid model make g_A large enough to already be in marginal conflict with the Oxford and Washington experiments. Furthermore, as can be seen in Fig. 8, measurements of the polarized-electron deuteron scattering asymmetry at different values of y should clearly distinguish the hybrid and WS models (it can already be said that the hybrid model is in some conflict with the $y = 0.21$ measurement).

The three varieties of νe scattering lead to an allowed region in the $g_A - g_V$ plot as shown in Fig. 10. The WS model with $\sin^2\theta_W = 0.2$–0.3

is clearly consistent with the data. Using the single Z^0 boson assumption, one can also plot the regions allowed by the two types of parity violation experiments.

The SLAC data rule out that version of the $SU(2)_L \times SU(2)_R \times U(1)$ model which predicted no parity-violation (to lowest order); however, other versions of that model reproduce the WS model's predictions for all neutral-current phenomena.

IV. CONCLUSIONS

The discussion in Sections II and III indicated that most models are ruled out by present analyses, but that the WS model and certain corresponding $SU(2) \times U(1) \times G$ models survive. In general, those models which fail are ruled out by many standard deviations. In contrast, the $SU(2) \times U(1)$ model of Weinberg and Salam agrees within 90% confidence levels with 17 different experimental numbers as shown in the Table. Note that at the 90% confidence level one would expect about 2 of the 17 numbers to disagree with the theory; the fact that none disagrees may indicate that the error bars are conservative. Clearly one should not use only one standard deviation since then 6 numbers would be expected to disagree with theory. Left out of the Table are the results from the atomic parity-violation experiments since there are conflicting experimental results.

If one chooses to believe both the Oxford-Washington result and the SLAC result (and assuming there is no large y dependence), then the standard WS model fails. However, there is a simple extension[28] of the model which can account for all of these phenomena. Consider the group $SU(2) \times U(1) \times U(1)_R$ where neutrinos are neutral under $U(1)_R$. Then all

TABLE

Comparison of WS Theory with Experiment. The theoretical numbers for exclusive pion production contain 30% errors as discussed in the text.

Process	Quantity Measured	90% Confidence Experimental Limits (Statistical + Systematics)	WS Theory $\sin^2\theta_W = 0.25$
$\nu N \to \nu X$	R	.295 ± .02	.31
$\bar{\nu} N \to \bar{\nu} X$	R	.34 ± .05	.36
$\nu N \to \nu \pi X$	N_{π^+}/N_{π^-}	.77 ± .22	.82
$\bar{\nu} N \to \bar{\nu} \pi X$	N_{π^+}/N_{π^-}	1.64 ± .58	1.18
$\nu p \to \nu p$	R	.11 ± .05	.11
$\bar{\nu} p \to \bar{\nu} p$	R	.19 ± .10	.12
$\nu p \to \nu p \pi^0$	R	.56 ± .16	.42 ± .13
$\nu n \to \nu n \pi^0$	R	.34 ± .15	.43 ± .13
$\nu n \to \nu p \pi^-$	R	.45 ± .20	.28 ± .08
$\nu p \to \nu n \pi^+$	R	.34 ± .12	.28 ± .08
$\bar{\nu} N \to \bar{\nu} N \pi^0$	R	.57 ± .16	.39 ± .12
$\bar{\nu} n \to \bar{\nu} p \pi^-$	R	.58 ± .26	.29 ± .09
$\nu_\mu e \to \nu_\mu e$	$\frac{\sigma}{E}\left(\frac{cm^2}{GeV}\right)$	$(1.5 \pm 1.5) \times 10^{-42}$	1.4×10^{-42}
$\bar{\nu}_\mu e \to \bar{\nu}_\mu e$	$\frac{\sigma}{E}\left(\frac{cm^2}{GeV}\right)$	$(1.9 \pm 1.8) \times 10^{-42}$	1.4×10^{-42}
$\bar{\nu}_e e \to \bar{\nu}_e e (1.5 < E_e < 3.0)$	$\sigma\ (cm^2)$	$(5.96 \pm 2.7) \times 10^{-43}$	5.94×10^{-43}
$\bar{\nu}_e e \to \bar{\nu}_e e (3.0 < E_e < 4.5)$	$\sigma\ (cm^2)$	$(3.21 \pm 1.3) \times 10^{-43}$	2.53×10^{-43}
$e_{pol}\ D \to e\ X$	A/Q^2	$(9.5 \pm 2.6) \times 10^{-5}$	7.2×10^{-5}

charged-current interactions and all neutrino interactions are unaffected. The parity-violation experiments here reflect the current

$$J_\mu^{WS} + \rho J_\mu^{I=0} \tag{4.1}$$

where the current resulting from $U(1)_R$ is isoscalar ($\bar{u}u + \bar{d}d$), and ρ is a free parameter which is taken to be small (say 0.1 or 0.2). Since the SLAC result involves differences between u_L and d_L (u_R and d_R), it is little affected by an isoscalar piece (which is multiplied by a small number). However, in the bismuth experiment one measures sums of u_L and d_L, and one finds that it is possible to cancel the effect due to the WS current. While it is possible to achieve this cancellation, it might seem to be a rather artificial or "unnatural" solution to this problem—obtaining zero by cancelling two large numbers against each other.

For the time, it might be best to wait for further atomic physics results on bismuth, thallium and hydrogen before reaching final conclusions. Nonetheless, the essential nature of the weak neutral-current interactions has become quite clear and the success of the Weinberg-Salam model is evident.

ACKNOWLEDGMENTS

The work described here was completed with Larry Abbott. I have benefited from discussions with S. Adler, J. Bjorken, F. Gilman, B. Kayser, W. Kozanecki, W. Marciano, J. Marriner, C. Matteuzzi, E. Monsay, F. Nezrick, Y.-J. Ng, E. Paschos, B. Roe, D. Sidhu, J. Strait, L. Sulak, S. Weinberg, and T. C. Yang. I would like to thank the Aspen Center for Physics (where this talk was prepared) and the Brookhaven National Laboratory theory group (where the written version was prepared) for the stimulating atmosphere each provided and for their hospitality.

REFERENCES

1. L. F. Abbott and R. M. Barnett, Phys. Rev. Lett. 40, 1303 (1978) and SLAC-PUB-2136 (1978) (submitted to Physical Review D). There are many other general discussions of neutral currents; among them are: D. P. Sidhu and P. Langacker, report No. BNL-24393 (1978) and Phys. Lett. 74B, 233 (1978); E. A. Paschos, report No. BNL-24619 (1978) and Phys. Rev. D15, 1966 (1977); F. E. Paige et al., Phys. Rev. D15, 3416 (1977); B. Kayser, NSF report (1978), invited talk at Int. Conf. on Neutrino Physics and Neutrino Astrophysics, Lafayette, Ind., April 28 – May 2, 1978; J. J. Sakurai, report No. UCLA/78/TEP/18 (1978), invited talk at Topical Conf. on Neutrino Physics at Accelerators, Oxford, England, July 4-9, 1978; UCLA/78/TEP/9 (1978), presented at Current Trends in Theory of Fields – 50 years of the Dirac Equation, Tallahassee, Fla., April 6-7, 1978; UCLA/77/TEP/23 (1977), presented at Irvine Conf. on Leptons and Quarks, Irvine, CA, Dec. 2-3, 1977; UCLA/77/TEP/15 (1977), invited talk at Neutrino 77, Elbrus, USSR, June 18-24, 1977; UCLA/76/TEP/21 (1976), invited lectures at Int. School of Subnuclear Physics, Erice, Sicily, June 23 – Aug. 8, 1976; Phys. Rev. Lett. 35, 1037 (1976); in Proc. 4th Int. Conf. on Neutrino Physics and Astrophysics, Dowington, PA., Apr. 26-28, 1974; P. Q. Hung and J. J. Sakurai, Phys. Lett. 72B, 208 (1977), 69B, 323 (1977) and 63B, 295 (1976); G. Ecker, Phys. Lett. 72B, 450 (1978); R. E. Hendrick and L.-F. Li, Carnegie-Mellon report (June 1978); see also Ref. 5, 7 and 10.

2. S. Weinberg, Phys. Rev. Lett. 19, 1264 (1967); A. Salam, in Elementary Particle Physics: Relativistic Groups and Analyticity, edited by N. Svartholm (Almquist and Wiksell, Stockholm, 1968), p. 367.

3. S. L. Glashow, J. Iliopoulos and L. Maiani, Phys. Rev. D2, 1285 (1970).

4. M. Holder et al. (CDHS), Phys. Lett. 72B, 254 (1977); J. Blietschau et al. (Gargamelle), Nucl. Phys. B118, 218 (1977); A. Benvenuti et al. (HPWF), Phys. Rev. Lett. 37, 1039 (1976); P. Wanderer et al. (HPWF), Phys. Rev. D17, 1979 (1978); F. S. Merritt et al. (CF), Phys. Rev. D17, 2199 (1978); P. C. Bosetti et al. (BEBC), Phys. Lett. 76B, 505 (1978).

5. L. M. Sehgal, Phys. Lett. 71B, 99 (1977); P. Q. Hung, Phys. Lett. 69B, 216 (1977); P. Scharbach, Nucl. Phys. B82, 155 (1974); and Ref. 1; recent work: S. Sarkar, Pennsylvania preprint, July 1978.

6. H. Kluttig et al., Phys. Lett. 71B, 446 (1977); J. Marriner, report No. LBL-6438 (1977), Univ. of California Ph. D. Thesis; B. Roe, invited talk at the Topical Conf. on Neutrino Physics at Accelerators, Oxford, England, July 4-9, 1978.

7. Analyses of elastic scattering have been done by S. Weinberg, Phys. Rev. D5, 1412 (1972); M. Barnett, Phys. Rev. D14, 2990 (1976); C. H. Albright et al., Phys. Rev. D14, 1780 (1976); V. Barger and D. V. Nanopoulos, Nucl. Phys. B124, 426 (1977); D. P. Sidhu, Phys. Rev. D14, 2235 (1976); F. Martin, Nucl. Phys. B104, 111 (1976); J. J. Sakurai and L. F. Urrutia, Phys. Rev. D11, 159 (1975).

8. L. Sulak, Harvard report, to appear in the Proc. of the Neutrinos-78 Conf., Purdue University, April 28 - May 2, 1978; J. B. Strait and W. Kozanecki, Harvard University Ph. D. theses (1978); D. Cline et al., Phys. Rev. Lett. 37, 252 and 648 (1976); see also W. Lee et al., Phys. Rev. Lett. 37, 186 (1976); M. Pohl et al., Phys. Lett. 72B, 489 (1978).

9. W. Krenz et al., report No. CERN/EP/PHYS 77-50 (1977); O. Erriques et al., Phys. Lett. 73B, 350 (1978); see also S. J. Barish et al., Phys. Rev. Lett. 33, 448 (1974); W. Lee et al., Phys. Rev. Lett. 38, 202 (1977).

10. S. L. Adler, Ann. Phys. 40, 189 (1968), and Phys. Rev. D12, 2644 (1975); S. L. Adler et al., Phys. Rev. D12, 3501 (1975) and Phys. Rev. D13, 1216 (1976); see also E. H. Monsay, Argonne report ANL-HEP-PR-78-08 (1978); G. Ecker in Ref. 7; and Ref. 1.

11. R. M. Barnett, Phys. Rev. Lett. 34, 41 (1975), Phys. Rev. D11, 3246 (1975); P. Fayet, Nucl. Phys. B78, 14 (1974); F. Gürsey and P. Sikivie, Phys. Rev. Lett. 36, 775 (1976); P. Ramond, Nucl. Phys. B110, 214 (1976).

12. R. M. Barnett, Phys. Rev. D13, 671 (1976).

13. A. De Rújula et al., Phys. Rev. D12, 3589 (1976); F. A. Wilczek et al., Phys. Rev. D12, 2768 (1975); H. Fritzsch et al., Phys. Lett. 59B, 256 (1975); S. Pakvasa et al., Phys. Rev. Lett. 35, 702 (1975).

14. R. M. Barnett, Phys. Rev. D15, 675 (1977).

15. B. W. Lee and S. Weinberg, Phys. Rev. Lett. 38, 1237 (1977); B. W. Lee and R. E. Shrock, Phys. Rev. D17, 2410 (1978); G. Segre and J. Weyers, Phys. Lett. 65B, 243 (1976).

16. R. M. Barnett and L. N. Chang, Phys. Lett. 72B, 233 (1977); R. M. Barnett et al., Phys. Rev. D17, 2266 (1978); P. Langacker and G. Segrè, Phys. Rev. Lett. 39, 259 (1977).

17. J. Pati and A. Salam, Phys. Rev. D10, 275 (1974); H. Fritzsch and P. Minkowski, Nucl. Phys. B103, 61 (1976); R. N. Mohapatra and D. P. Sidhu, Phys. Rev. Lett. 38, 667 (1977); A. De Rújula, H. Georgi and S. L. Glashow, Ann. Phys. 109, 242 and 258 (1977).

18. H. Georgi and S. Weinberg, Phys. Rev. D17, 275 (1978); R. Gatto and F. Strocchi, Geneva report (1978).

19. P. E. G. Baird et al., Nature 264, 528 (1976).

20. N. Fortson, to appear in the Proc. of the Neutrinos-78 Conf., Purdue University, April 28 - May 2, 1978; E. Henley ibid.; W. J. Marciano and A. I. Sanda, Phys. Rev. D17, 3055 (1978) and Rockefeller report No. COO-2232B-153 (1978); G. Feinberg, Columbia report No. CU-TP-111, to appear in the Proc. of the Ben Lee Memorial Int. Conf., Batavia, Ill., Oct. 20-22, 1977

21. P. G. H. Sandars, in Proc. 1977 Int. Symp. on Lepton and Photon Interactions at High Energies, edited by F. Gutbrod (DESY, Hamburg, 1977) p. 599.

22. L. M. Barkov and M. S. Zolotorev, Pisma Zh. Eksp. Teor. Fiz. (JETP Lett) 26, 379 (1978).

23. F. J. Hasert et al., Phys. Lett. 46B, 121 (1973); J. Blietschau et al., Nucl. Phys. B114, 189 (1976); M. Faissner et al., Phys. Rev. Lett. 41, 213 (1978); A. M. Cnops et al., Phys. Rev. Lett. 41, 357 (1978); P. Alibran et al., Phys. Lett. 74B, 422 (1978); F. Reines et al., Phys. Rev. Lett. 37, 315 (1976).

24. C. Y. Prescott et al., report No. SLAC-PUB-2148 (1978).

25. R. N. Cahn and F. J. Gilman, Phys. Rev. D17, 1313 (1978) and references therein.

26. J. D. Bjorken, report No. SLAC-PUB-2146 (1978).

27. W. J. Marciano and A. I. Sanda, Rockefeller report No. COO-2232B-142 (1976).

28. Private communications from J. D. Bjorken and T. C. Yang. It is possible that other people have also considered such an extension and its application to these two experiments.

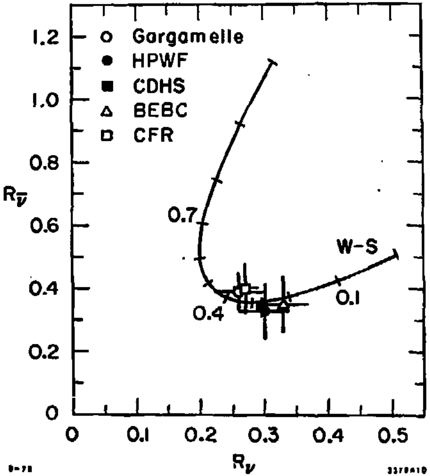

Fig. 1. The ratio of neutral to charged-current deep-inelastic scattering cross sections for antineutrinos versus that ratio for neutrinos. The curve shows the predictions of the WS model as a function of $\sin^2\theta_W$ (each tick mark indicates a tenth value of $\sin^2\theta_W$). The data are from Ref. 4.

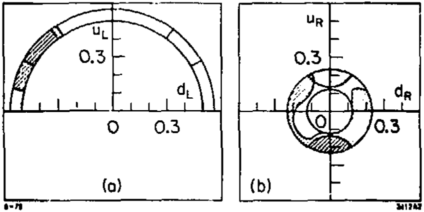

Fig. 2. The left (a) and right (b) coupling-constant planes. The lower half of (a) is omitted due to our sign convention $u_L \geq 0$. The annular regions are allowed by deep-inelastic data. The regions shaded with dots are allowed by inclusive-pion results, and the region shaded with lines is allowed by elastic and exclusive-pion data. Unique determination of the quark coupling values is given by the region shaded with both dots and lines.

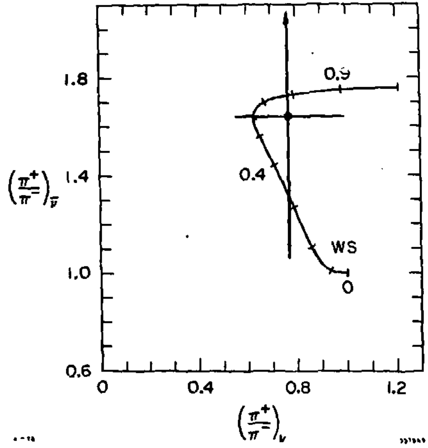

Fig. 3. The ratio of π^+ to π^- multiplicities from inclusive-pion data for antineutrinos versus that ratio for neutrinos. The curve shows the predictions of the Weinberg-Salam model as a function of $\sin^2\theta_W$. The data are from Ref. 5, and 90% confidence limits are shown.

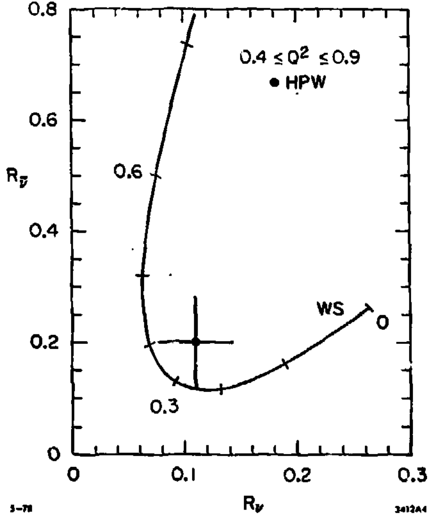

Fig. 4. The ratio of neutral to charged-current elastic νp scattering cross sections for antineutrinos versus that ratio for neutrinos where $0.4 \le Q^2 \le 0.9$ GeV^2. The curve shows the predictions of the Weinberg-Salam model as a function of $\sin^2\theta_W$. The data are from Ref. 8, and only statistical uncertainties are shown (at the 90% confidence level).

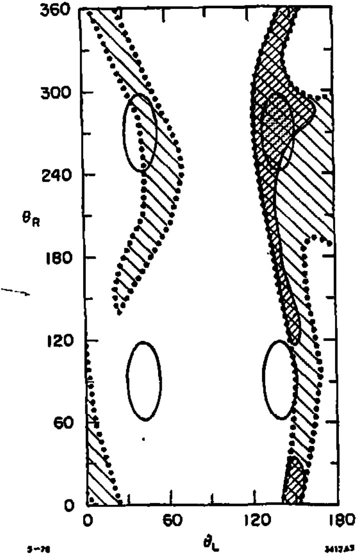

Fig. 5. The allowed angles in the coupling planes of Fig. 2 for fixed radii taken at the center of the allowed annulus (r_L = 0.53) in the left-coupling plane and at the outer edge of the allowed annulus (r_R = 0.22) in the right-coupling plane. The ellipses indicate the regions allowed by inclusive-pion data; going clockwise from the upper-right, they are regions A, B, C and D, respectively. The area shaded with lines and enclosed with a dotted curve is allowed by elastic data. The region which is cross-hatched is allowed by elastic and exclusive-pion results. The area shaded with dots is the only region allowed by all data.

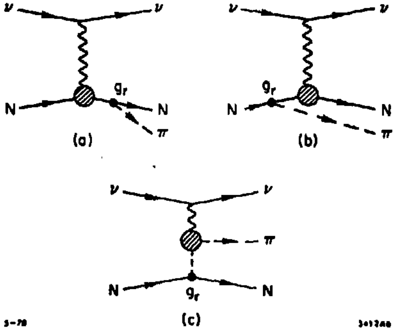

Fig. 6. Born diagrams for the exclusive-pion-production analysis. g_r is the pion-nucleon coupling constant.

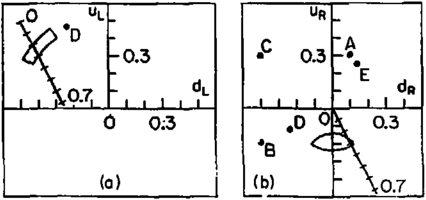

8 - 78 3184A2

Fig. 7. Various gauge models compared with the allowed coupling-constant region. The lines mark the Weinberg-Salam model for values of $\sin^2\theta_W$ from 0.0 to 0.7. The points labeled A-E are the predictions of various models discussed in the text. For A, B, C, and E, u_L and d_L lie within the allowed region in the left-coupling plane.

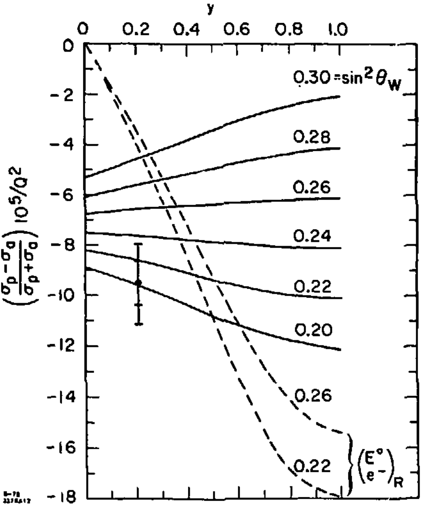

Fig. 8. The asymmetry in the SLAC experiment in which polarized electrons are inelastically scattered off deuterons, shown as a function of $y \equiv (E_e - E_e')/E_e$. The solid (dashed) curves are the predictions of the WS ("hybrid") model for various values of $\sin^2\theta_W$. The data are from Ref. 24 and have $Q^2 = 1.6$ GeV^2 and $y = 0.21$. σ_p and σ_a refer to cross sections for electrons polarized parallel and antiparallel to the beam.

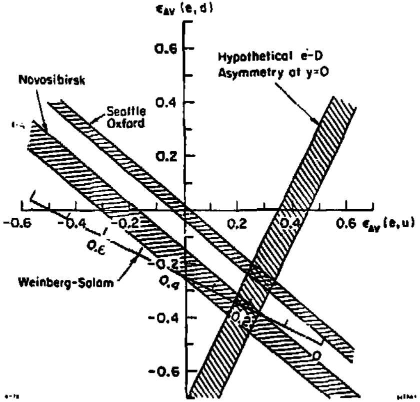

<u>Fig. 9.</u> Allowed values of $\epsilon_{AV}^{e,q}$, <u>assuming</u> that the measured deep-inelastic polarized-electron deuteron scattering asymmetry represents its value at y = 0.

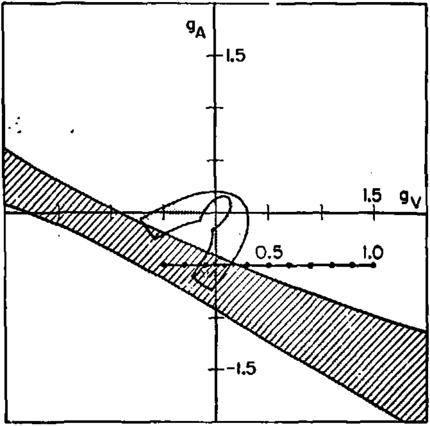

Fig. 10. Ninety percent confidence limits on g_A and g_V of the electron. The horseshoe-shaped area at the center of the figure is the overlap region allowed by the three types of νe scattering experiments. The band shaded with lines is the allowed region from the SLAC polarized-electron-deuteron scattering experiment (Ref. 24) assuming a single Z^0 boson and values from Sec. II of quark couplings (including quark error bars). The upper (lower) band shaded with dots is for the Washington-Oxford (Novosibirsk) parity-violation experiments. The predictions of the WS model are shown for tenth values of $\sin^2\theta_W$.

SLAC-PUB-2183
August 1978
(T/E)

WEAK NEUTRAL-CURRENT INTERACTIONS*†

R. Michael Barnett
Stanford Linear Accelerator Center
Stanford University, Stanford, California 94305

I. INTRODUCTION

The structure of gauge theories of the weak and electromagnetic interactions can be studied with the weak neutral-current interactions of quarks and leptons. In gauge theories, the charged currents (CC) are related to the neutral currents (NC). In SU(2) × U(1) models, for example, the determination of the neutral currents follows from the relation (where for simplicity right-handed charged currents are ignored):

$$J_\mu^{NC} = \bar{q}\, C^0\, \gamma_\mu\, (1 + \gamma_5)\, q - 2\, \sin^2\theta_W\, J_\mu^{em} \qquad (1.1)$$

where q is the vector (u, c, d, s, ...) and J_μ^{em} is the electromagnetic current. C^0 is a matrix obtained from

$$C^0 = \left[C, C^\dagger\right] \qquad (1.2)$$

where C is a matrix giving the appropriate charged current of a given SU(2) × U(1) model, i.e.,

$$J_\mu^{CC} = \bar{q}\, C\, \gamma_\mu\, (1 + \gamma_5)\, q. \qquad (1.3)$$

Thus information about neutral currents can determine the existence or non-existence of charged currents such as $\bar{u}b_R$, $\bar{t}d_R$ or $\bar{E}^0 e_R$ where m_t, m_b and m_{E^0} can be arbitrarily large.

*Research supported in part by the Department of Energy.

†Invited talk at the Summer Institute on Particle Physics, Weak Interactions - Present and Future, Stanford Linear Accelerator Center, Stanford, California, July 10-21, 1978.

With the data now available, it is possible to establish uniquely the values of the neutral-current couplings of u and d quarks. The roles of each type of experiment in the determination of these couplings are analyzed in Section II. The section concludes with a discussion of the implications of these results for gauge models of the weak and electromagnetic interactions. Section III contains an analysis of the neutral-current couplings of electrons. The first part of this section presents an analysis of the data based on the assumption that only one Z^0 boson exists. The second part discusses a model-independent analysis of parity-violation experiments. The conclusions are given in Section IV.

II. DETERMINATION OF QUARK COUPLINGS

A model-independent analysis[1] of neutrino scattering data has shown that the neutral-current couplings of u and d quarks could be uniquely determined. The input involved four types of experiments which will be discussed separately. The work[1] described here was done together with Larry Abbott.

It is assumed here that there are only V and A currents. The currents of s and c quarks are neglected. The notation used in this section has u_L, d_L, u_R and d_R (L ≡ left and R ≡ right) as the coefficients in the effective neutral-current coupling:

$$\mathscr{L} = \frac{G}{\sqrt{2}} \bar{\nu}\gamma_\mu(1 + \gamma_5)\nu\Big[u_L\, \bar{u}\gamma_\mu\, (1 + \gamma_5)u + u_R\, \bar{u}\gamma_\mu\, (1 - \gamma_5)\, u + d_L\, \bar{d}\gamma_\mu\, (1 + \gamma_5)\, d + d_R\, \bar{d}\, \gamma_\mu\, (1 - \gamma_5)\, d\Big] \qquad (2.1)$$

In the Weinberg-Salam (WS) model[2] with the Glashow-Iliopoulos-Maiani (GIM) mechanism[3] incorporated, u_L is equal to $\frac{1}{2} - \frac{2}{3}\sin^2\theta_W$ with θ_W a free parameter of the theory; u_R, d_L and d_R have similar forms.

Note that there is no assumption about the bosons carrying the neutral current, only an assumption that the effective Lagrangian (2.1) holds.

A. Neutrino-Nucleon Inclusive Scattering

The calculation of deep-inelastic neutrino scattering off nucleons ($\nu N \to \nu X$) is done using the parton model. For sake of discussion only, let us neglect sea contributions and scaling violations (from QCD). For an isoscalar target, one finds that the neutral-current (NC) and charged-current (CC) cross sections for neutrinos are:

$$\sigma_\nu^{NC} = \frac{G^2 mE}{\pi} \int dx\, F(x) \left[\left(u_L^2 + d_L^2\right) + \frac{1}{3}\left(u_R^2 + d_R^2\right)\right] \qquad (2.2)$$

$$\sigma_\nu^{CC} = \frac{G^2 mE}{\pi} \int dx\, F(x) \,[1] \qquad (2.3)$$

Then the ratios for neutrinos and for antineutrinos are

$$R_\nu \equiv \frac{\sigma^{NC}}{\sigma^{CC}} = \frac{\left(u_L^2 + d_L^2\right) + \frac{1}{3}\left(u_R^2 + d_R^2\right)}{(1)} \qquad (2.4)$$

$$R_{\bar\nu} \equiv \frac{\sigma^{NC}}{\sigma^{CC}} = \frac{\frac{1}{3}\left(u_L^2 + d_L^2\right) + \left(u_R^2 + d_R^2\right)}{\left(\frac{1}{3}\right)} \qquad (2.5)$$

Therefore, one can determine the values of $\left(u_L^2 + d_L^2\right)$ and of $\left(u_R^2 + d_R^2\right)$, which are the radii in the left (L) and right (R) coupling planes. The available data[4] are shown in Fig. 1 along with the predictions of the WS model.

Using the data[4] of the CERN-Dortmund-Heidelberg-Saclay (CDHS) group ($R_\nu = 0.295 \pm 0.01$ and $R_{\bar\nu} = 0.34 \pm 0.03$), the values of the radii in the L and R planes allowed at the 90% confidence level are shown in Fig. 2.

An overall sign ambiguity among the four couplings is resolved by requiring $u_L > 0$.

B. Inclusive Production of Pions by Neutrinos

The allowed radii are well determined by deep-inelastic scattering. It remains to determine the allowed angles in the left and right planes. Let us define

$$\theta_L \equiv \arctan\ (u_L/d_L)$$
$$\theta_R \equiv \arctan\ (u_R/d_R) \qquad (2.6)$$

One means of determining the angles is through use of inclusive pion production ($\nu N \rightarrow \pi X$). Again parton model assumptions are involved in the calculations. This analysis has been discussed by Sehgal, Hung and Scharbach.[5] It is assumed that pions produced in the current-fragmentation region (leading pions) are decay products of the struck quark. If z is defined as E_π/E_{had} (where E_{had} = [total hadron energy] = energy of the struck quark), then $D_q^\pi(z)$ describes the probability that a given pion has a fraction z of energy of the struck quark q. The calculations are similar to those for inclusive deep-inelastic scattering except that the limited specification of the final state requires that the u couplings be multiplied by $D_u^\pi(z)$ and d couplings by $D_d^\pi(z)$. Then the ratio of π^+ to π^- production for neutrinos is (neglecting sea contributions for discussion only):

$$\frac{N_{\pi^+}}{N_{\pi^-}} = \frac{\left(u_L^2 + \frac{1}{3}\,u_R^2\right) F_u^{\pi^+} + \left(d_L^2 + \frac{1}{3}\,d_R^2\right) F_d^{\pi^+}}{\left(u_L^2 + \frac{1}{3}\,u_R^2\right) F_u^{\pi^-} + \left(d_L^2 + \frac{1}{3}\,d_R^2\right) F_d^{\pi^-}}\,. \qquad (2.7a)$$

with

$$P_q^\pi \equiv \int_{z_1}^{z_2} dz\, D_q^\pi \tag{2.7b}$$

where one requires $z > z_1$ (leading pions), $z < z_2$ (avoids resonance region) and $E_{had} > E_0$; the values of z_1, z_2, and E_0 depend on the particular experiment.

There are isospin relations

$$D_u^{\pi^+} = D_d^{\pi^-} \qquad \text{and} \qquad D_u^{\pi^-} = D_d^{\pi^+} \tag{2.8}$$

which help simplify Eq. (2.7). Furthermore, the ratio of $D_u^{\pi^+}$ to $D_u^{\pi^-}$ can be measured in ep scattering and in charged-current neutrino scattering; the relevant ratio is

$$\eta \equiv \int_{z_1}^{z_2} dz\, D_u^{\pi^+}(z) \bigg/ \int_{z_1}^{z_2} dz\, D_u^{\pi^-}(z) \tag{2.9}$$

Using Eq. (2.8) and (2.9) in Eq. 2.7, one obtains

$$\left(\frac{N_{\pi^+}}{N_{\pi^-}}\right)_\nu = \frac{\left(u_L^2 + \frac{1}{3}u_R^2\right)\eta + \left(d_L^2 + \frac{1}{3}d_R^2\right)}{\left(u_L^2 + \frac{1}{3}u_R^2\right) + \left(d_L^2 + \frac{1}{3}d_R^2\right)\eta} \tag{2.10}$$

For antineutrinos, Eq. (2.10) holds if one interchanges L and R. There are corrections to Eq. (2.10) from sea contributions and from experimental efficiencies.

The data used here are low energy data from Gargamelle[6] at the CERN PS. These data are $\left(N_{\pi^+}/N_{\pi^-}\right)_\nu = 0.77 \pm 0.14$ and $\left(N_{\pi^+}/N_{\pi^-}\right)_{\bar\nu} = 1.64 \pm 0.36$ for $0.3 < z < 0.7$ and $E_{had} > 1$ GeV. These are shown in Fig. 3

along with the predictions of the WS model.

Recently, high energy data have become available. The neutrino data[6] are not for pions but for all charged particles (within the prescribed cuts); Abbott and I have used electroproduction data to estimate K and p contamination in the signal and find that the results are consistent with the Gargamelle results. The preliminary antineutrino data[6] are also consistent with the low energy data.

We find that the high energy data do not change our conclusions or the final values of the neutral-current couplings obtained from our analysis. However, the error bars would be increased; this is due in part to the fact that the actual quantity used (see Eq. B3 and B4 in the second paper of Ref. 1) involves differences between numbers of the same magnitude.

As can be seen in Fig. 2, the Gargamelle pion-inclusive data (even with 90% confidence levels) place severe restrictions on the allowed angles. However, since the ratios (Eq. 2.10) are functions of the squares of the couplings, there are various sign ambiguities.

C. Elastic Neutrino-Proton Scattering

Further determination of the allowed angles along with resolution of some sign ambiguities can be obtained from analysis[1,7] of elastic neutrino-proton scattering ($\nu p \to \nu p$). Unlike the calculations of Sections IIA and B, no parton model assumptions are needed here. The matrix element for the process is

$$\langle p' | J_\mu | p \rangle = \bar{u}(p') \left[\gamma_\mu F_1 + \frac{i\sigma_{\mu\nu} q^\nu}{2m} F_2 + \gamma_5 \gamma_\mu F_A \right] u(p) \qquad (2.11)$$

The vector form factors $\left[F_1(q^2) \text{ and } F_2(q^2) \right]$ are related via CVC to the electromagnetic form-factors of protons and neutrons:

$$\text{Isovector}\quad F_i = F_i^p - F_i^n \tag{2.12}$$

$$\text{Isoscalar}\quad F_i = F_i^p + F_i^n \tag{2.13}$$

The isovector part of the axial-vector form-factor has been measured and has the form:

$$F_A(q^2) = \frac{1.23}{(1 + Q^2/m_A^2)^2} \tag{2.14}$$

where $m_A^2 \approx 0.79\ \mathrm{GeV}^2$ (our results are not very sensitive to variation of m_A). The isoscalar part of the axial-vector form factor is assumed to have the same Q^2 dependence.

The appropriate factors between these four terms are obtained using the SU(6) wavefunctions of nucleons. The data of the Harvard-Pennsylvania-Wisconsin (HPW) group[8] are $R_\nu \equiv \sigma^{NC}/\sigma^{CC} = 0.11 \pm 0.02$ and $R_{\bar{\nu}} = 0.19 \pm 0.05$ (statistical errors shown). These are shown in Fig. 4 along with the predictions of the WS model.

The resolution of the sign ambiguities remaining from the pion-inclusive data is difficult to see in Fig. 2, since correlations between the left and right planes are not evident. From the pion-inclusive data shown in Fig. 2, one might think that there are 2, 3, or 4 allowed regions. The correlations can be made evident by plotting θ_L vs θ_R (see Eq. 2.6) as in Fig. 5; this can be done "uniquely," because the radii in the left and right planes are well determined. The pion-inclusive data result in four allowed regions (appearing as ellipses in Fig. 5); there would be eight regions except that $d_R \approx 0$ so that four pairs of regions coalesce.

By "inverting" the νp elastic scattering data (with the analysis described above), one can rule out two of these four regions completely and can rule out substantial portions of one other. Varying portions of two regions do remain allowed. Independent of the pion-inclusive data, the elastic data severely limit the allowed regions in coupling space.

D. Production of Exclusive Pion Modes by Neutrinos

Two of the three remaining allowed regions in Fig. 5 can be ruled out by consideration of the cross-section ratios for six exclusive channels containing a pion:

$$\sigma(\nu p \to \nu p\pi^o)/\sigma_1 \qquad (2.15)$$

$$\sigma(\nu n \to \nu n\pi^o)/\sigma_1 \qquad (2.16)$$

$$\sigma(\nu n \to \nu p\pi^-)/\sigma_1 \qquad (2.17)$$

$$\sigma(\nu p \to \nu n\pi^+)/\sigma_1 \qquad (2.18)$$

$$\left[\sigma(\bar{\nu}p \to \bar{\nu}p\pi^o) + \sigma(\bar{\nu}n \to \bar{\nu}n\pi^o)\right]/\sigma_2 \qquad (2.19)$$

$$\sigma(\bar{\nu}n \to \bar{\nu}p\pi^-)/\sigma_2 \qquad (2.20)$$

with

$$\sigma_1 \equiv \sigma(\nu n \to \mu^- p\pi^o) \qquad (2.21)$$

$$\sigma_2 \equiv \sigma(\bar{\nu}p \to \mu^+ n\pi^o) \qquad (2.22)$$

where recent Gargamelle data[9] were used.

To analyze the data, the detailed pion-production model developed by Adler[10] was used. This model is superior to all other pion-production models; it includes non-resonant production (an important feature), incorporates excitation of the $\Delta(1232)$ resonance, and satisfies current algebra constraints. The model gives quite good descriptions of a variety of data and is crucial for analysis of the Gargamelle data.

One begins with the Born amplitudes shown in Fig. 6 which are given in terms of the form factors F_1, F_2 and F_A (described in Section IIIC), F_π (coming from Fig. 6c) and g_π (the pion-nucleon coupling). There are two types of corrections applied.

One comes from using the current algebra relation:

$$T\left\{\partial^\mu J_\mu^5 \mathcal{J}\right\} = -\delta\ (x_0)\left[J_0^5, \mathcal{J}\right] + \partial^\mu\ T\left\{J_\mu^5 \mathcal{J}\right\} \tag{2.23}$$

(where T indicates time-ordered product, and $\mathcal{J}$ is the weak current of interest). Taking the Fourier transforms and then the matrix element between nucleon states for each piece of Eq. (2.23, one finds from PCAC that the left side is proportional to the desired matrix element $\langle N\pi|\mathcal{J}(0)|N\rangle$. The first term on the right side leads to additional form factor terms. The second term containing the J^5 current with axial-vector couplings, rather than the pseudo-scalar coupling assumed for the pion, implies certain vertex corrections.

The second type of correction is for final-state interactions; the outgoing pion and nucleon can resonate. In particular, for the appropriate $I = \frac{3}{2}$ terms, one must account for the Δ(1232) resonance. There are the usual phase shifts ($e^{i\delta_R}$) and enhancement effects for this P_{33} resonance. It is <u>crucial</u> to keep the non-resonant (including $I = \frac{1}{2}$) pieces; both the analysis and the data say those pieces are significant.

To avoid other (higher mass) resonances and for consistency with the soft-pion assumptions of current algebra, it is necessary to require that the invariant mass W of the pion-nucleon system be less than 1.4 GeV. Unfortunately, the data are not available with this cut, and for modes with final-state neutrons it is, of course, quite difficult to obtain the invariant mass. However, the relevance of the cut to our conclusions is minimized because: (1) most data are below the W = 1.4 GeV cut; (2) ratios of cross sections are used; (3) application of the cut to the limited experimental mass plots available indicates a strengthening of our conclusions; and (4) the model predictions are assumed to be valid only to within 30% and the data to the 90% confidence level (this is somewhat different from the procedure followed in the first paper of Ref. 1). This fourth point is approximately equivalent to allowing any theoretical values which lie within a factor of two of the various data.

Our analysis of the six exclusive pion-production channels shows that small values of $\theta_L (\theta_L < 90^\circ)$ are totally forbidden by these data. Recall that there were four regions in Fig. 5 allowed by pion-inclusive data, and that two were ruled out by the elastic data. A third region (with $\theta_L \approx 40^\circ$ and $\theta_R \approx 270^\circ$ in Fig. 5) is now completely ruled out. The region with $\theta_L \approx 140^\circ$ and $\theta_R \approx 90^\circ$, which was forbidden by elastic data, is not allowed by these data either. The exclusion of this latter region by these data alone would be much more marginal than for the regions with $\theta_L \approx 40^\circ$. What remains is a single region (with $\theta_L \approx 140^\circ$ and $\theta_R \approx 270^\circ$) which is in good agreement with all four types of neutrino experiments. This unique determination can be expressed in terms of the coupling constants so that the allowed region (see Fig. 2) is

$$\begin{aligned} u_L &= 0.35 \pm 0.07 \qquad & u_R &= -0.19 \pm 0.06 \\ d_L &= -0.40 \pm 0.07 \qquad & d_R &= 0.0 \pm 0.11 \end{aligned} \tag{2.24}$$

where the errors are 90% confidence levels and an overall sign convention $(u_L \geq 0)$ has been assumed.

E. Implications for Gauge Models

In examining the structure of gauge models of weak and electromagnetic interactions, one of the important questions is whether, in the context of $SU(2) \times U(1)$ models, there is any evidence for right-handed charged currents. The neutral-current results are directly relevant to this question and indicate that there are no right-handed charged currents for u or d quarks in $SU(2) \times U(1)$ models.

This conclusion can be obtained by consideration of Fig. 7 which shows the allowed regions from Fig. 2. All $SU(2) \times U(1)$ models with the left-handed coupling doublet $\bar{u}d_L$ have values in the left-coupling plane (Fig. 7a) which are indicated by the line with tick marks. These models have $\sin^2 \theta_W$ as a free parameter so that the position on the line (i.e., the value of $\sin^2 \theta_W$) is determined solely from the data. Clearly from Fig. 7a, the allowed value of $\sin^2 \theta_W$ is between 0.2 and 0.3.

Now looking at the right coupling plane, Fig. 7b, one sees that for the WS model the values of $\sin^2 \theta_W = 0.2 - 0.3$ are also allowed there. The overall magnitude of these neutral-current couplings was dependent on the mass ratio of $m(Z^0)/m(W^\pm)$ which is predicted by the WS model[2] with the minimal Higgs boson structure (one or more doublets) to be:

$$m_{Z^0} = m_{W^\pm}/\cos \theta_W \tag{2.25}$$

If this mass ratio were not as predicted, then the model would be ruled out (for example, one might find that $\sin^2 \theta_W = 0.1$ was required by the left-coupling plane, Fig. 7a, but $\sin^2 \theta_W = 0.4$ by the right-coupling plane, Fig. 7b). The success of these predictions of the WS model is remarkable.

For other $SU(2) \times U(1)$ models, if one chooses $\sin^2 \theta_W = 0.3$ from the left-coupling plane, then the resulting points in the right plane are determined. Shown in Fig. 7b are the points for the cases where the models have the right-handed doublets $\bar{u}b_R$ (labeled A),[11] $\bar{c}d_R$ (B)[12], and both $\bar{u}b_R$ and $\bar{c}d_R$ (C). The latter model (C)[13] has been called the "vector" model. As can be seen, these models are ruled out by the data. Varying the ratio $m(Z^0)/m(W^{\pm})$ moves the points toward or away from the origin, but these models still cannot survive. There are other SU(2) × U(1) models[14] involving $-\frac{4}{3}$ and 5/3 charged quarks, and these are also ruled out.

The applicability of these results is <u>not</u> limited to SU(2) × U(1) models. For example, there are two SU(3) × U(1) models which are ruled out by these data. One[15] (labeled D in Fig. 7b) has the u quark in a right-handed singlet and the other[16] (E) has the u quark in a right-handed triplet (for this latter case the parameters of the model were chosen to place u_L and d_L in the allowed region in Fig. 7a).

These results also apply to the $SU(2)_L \times SU(2)_R \times U(1)$ model.[17] Since that model can be chosen to have the same values of u_L, d_L, u_R and d_R as the WS model, it is allowed by the analysis of quark couplings. In fact, Georgi and Weinberg[18] have generalized this conclusion by showing that at zero-momentum transfer, the neutral-current interactions of neutrinos in an SU(2) × G × U(1) gauge theory are the same as in the corresponding SU(2) × U(1) theory if neutrinos are neutral under G.

III. DETERMINATION OF ELECTRON COUPLING

A. Analysis of Neutrino and Parity Violation Experiments

There are two types of experiments which are used to obtain information about the weak neutral-current coupling of the electron. The first is neutrino-electron scattering which can be analyzed in a model-independent fashion as was done for quarks. The second involves searches for parity-violation in electron-nucleon interactions. This analysis requires use of the uniquely determined quark couplings obtained in Section II. However, if the results from analysis of parity-violation experiments are to be compared with those from νe scattering (i.e., if g_A and g_V are to be calculated), then one must make the assumption that there is only one Z^0 boson which can carry the relevant weak neutral currents.

One type of experiment involves the search for parity-violation in atomic transitions in bismuth. The details of these experiments have been given elsewhere.[19] Clearly such effects are proportional to the VA interference terms, and, in the case of bismuth, the $(V_{hadron}\, A_{electron})$ term is completely dominant. The optical rotation ρ which is measured is then proportional to this term, i.e., $\rho = KQ_w$, where K is a constant and (with the one Z^0 assumption)

$$Q_w = -4\, V_{had}\, g_A \tag{3.1}$$

If one defines e_L and e_R as the coefficients in the effective neutral-current coupling:

$$\mathscr{L} \propto \frac{G}{\sqrt{2}}\left[e_L\, \bar{e}\, \gamma_\mu(1+\gamma_5)\, e + e_R\, \bar{e}\, \gamma_\mu(1-\gamma_5) e\right] \tag{3.2}$$

then

$$\begin{aligned} g_A &\equiv (e_L - e_R) \\ g_V &\equiv (e_L + e_R) \end{aligned} \tag{3.3}$$

and

$$\begin{aligned} V_{had} = &(2u_L + d_L + 2u_R + d_R)Z \\ &+ (u_L + 2d_L + u_R + 2d_R)N \end{aligned} \tag{3.4}$$

where Z and N are the numbers of protons and neutrons (for bismuth, $Z = 83$ and $N = 126$).

Although there is some question[20] about the atomic and nuclear calculations of K (where $\rho = KQ_W$), present theoretical estimates for K are such that the optical rotations ρ for the two transitions that have been measured are

$$\rho \approx 1.1 \times 10^{-9}\ Q_W \text{ radians} \quad (\text{for } 8757\ \text{Å}) \tag{3.5}$$

$$\rho \approx 1.5 \times 10^{-9}\ Q_W \text{ radians} \quad (\text{for } 6476\ \text{Å}) \tag{3.6}$$

Two experiments report results consistent with zero: the Washington group[20] reports $\rho = (-0.5 \pm 1.7) \times 10^{-8}$ for the 8757 Å transition while the Oxford group[21] reports $\rho = (+2.7 \pm 4.7) \times 10^{-8}$ for the 6476 Å transition. By contrast, the Novosibirsk experiment[22] found $\rho = (-21 \pm 6) \times 10^{-8}$ for the 6476 Å transition.

Assuming that there exists only one Z^0 boson, then the quark couplings (Eq. 2.24) imply that $g_A \approx 0 \pm 0.06$ for the first two experiments, and $g_A \approx -0.4 \pm 0.17$ for the Novosibirsk experiment.

The other type of experiment for which results have been reported[23] involves νe elastic scattering (with $\nu_\mu e$, $\bar{\nu}_\mu e$ and $\bar{\nu}_e e$ measured by various groups). The cross sections for $\nu_\mu e$ and $\bar{\nu}_\mu e$ scattering are (no Z^0 assumption is involved here):

$$\frac{d\sigma^{\nu,\bar{\nu}}}{dE_e} = \frac{G\, m_e}{2\pi}\left[\left(g_V \pm g_A\right)^2 + \left(g_V \mp g_A\right)^2 \left(1 - \frac{E_e}{E_\nu}\right)^2 + \left(g_A^2 - g_V^2\right)\frac{m_e E_e}{E_\nu^2}\right] \tag{3.7}$$

where bottom signs are for antineutrinos. For $\bar{\nu}_e e$ elastic scattering, there is an annihilation term (through a W^- boson), so that in Eq. (3.7) $g_V \to g_V + 1$ and $g_A \to g_A + 1$. Knowledge of these cross sections leads to allowed regions in a g_A-g_V plot which are ellipsoidal annuli.

Results have been reported for a SLAC experiment[24] involving the deep-inelastic scattering of polarized electrons off deuterium and hydrogen targets. In this experiment one measures the asymmetry between the cross sections σ_p and σ_a with electrons polarized parallel and antiparallel to the beam. If there are weak parity-violating effects, the asymmetry will be non-zero. The asymmetry is sensitive to both the $V_{had}\,A_{elec}$ and $A_{had}\,V_{elec}$ terms, and furthermore involves no difficult atomic or nuclear calculations.

For an isoscalar target (deuterium) the asymmetry (see Ref. 25) is, with the one Z^0 assumption:

$$\frac{d\sigma_p - d\sigma_a}{d\sigma_p + d\sigma_p} = 64 \times 10^{-5}\, Q^2 \left\{\left[\frac{2}{3}(u_L + u_R) - \frac{1}{3}(d_L + d_R)\right] g_A + \left[\frac{1-(1-y)^2}{1+(1-y)^2}\right]\left[\frac{2}{3}(u_L - u_R) - \frac{1}{3}(d_L - d_R)\right] g_V\right\} \quad (3.8)$$

The SLAC experiment on the inelastic scattering of polarized electrons from deuterium has reported an asymmetry of $(-9.5 \pm 1.6) \times 10^{-5}\, Q^2$ where Q^2 is about 1.6 GeV^2 and $y = 0.21$. This is shown in Fig. 8 along with the predictions of the WS model and the "hybrid" model (described later). Similar results were obtained with hydrogen. A run at a higher value of y may be made in the future.

B. Model Independent Analysis of Parity Violation Experiments

Bjorken[26] has shown how to analyze parity violation experiments in a model-independent fashion (in particular, there is <u>no</u> need to assume that there is only one Z^0 boson). One defines the parity-violation parameters $\epsilon_{VA}^{e,q}$ and $\epsilon_{AV}^{e,q}$ as the coefficients in the effective Lagrangian

$$\mathcal{L} = \frac{G}{\sqrt{2}} \left[\bar{e}\gamma^{\mu} e \left\{ \epsilon_{VA}^{e,u} \bar{u}\gamma_{\mu}\gamma_5 u + \epsilon_{VA}^{e,d} \bar{d}\gamma_{\mu} \gamma_5 d \right\} + \bar{e}\gamma^{\mu} \gamma_5 e \left\{ \epsilon_{AV}^{e,u} \bar{u}\gamma_{\mu} u + \epsilon_{AV}^{e,d} \bar{d}\gamma_{\mu} d \right\} \right] \quad (3.9)$$

It turns out that more information can be obtained about $\epsilon_{AV}^{e,q}$ than about $\epsilon_{VA}^{e,q}$ from present data. The implications of the results of the Novosibirsk, Oxford and Washington experiments[20-22] in bismuth and of a "hypothetical" $y = 0$ polarized-electron deuterium experiment are shown in Fig. 9, along with the predictions of the WS model.

C. Implications for Gauge Models

The WS model predicts $g_A = -0.5$ (independent of $\sin^2 \theta_W$) which is not consistent with the results of the Oxford and Washington experiments, but it is consistent with the results of the Novosibirsk experiment. There is an SU(2) × U(1) model which predicts $g_A \approx 0$. This model, called the "hybrid" model, is identical to the WS model except that in addition to the coupling $(\bar{\nu}e)_L$ there is a right-handed coupling $(\bar{E^0}\, e)_R$. However, Marciano and Sanda[27] have shown that higher order corrections in the hybrid model make g_A large enough to already be in marginal conflict with the Oxford and Washington experiments. Furthermore, as can be seen in Fig. 8, measurements of the polarized-electron deuteron scattering asymmetry at different values of y should clearly distinguish the hybrid and WS models (it can already be said that the hybrid model is in some conflict with the $y = 0.21$ measurement).

The three varieties of νe scattering lead to an allowed region in the $g_A - g_V$ plot as shown in Fig. 10. The WS model with $\sin^2 \theta_W = 0.2$-0.3

is clearly consistent with the data. Using the single Z^0 boson assumption, one can also plot the regions allowed by the two types of parity violation experiments.

The SLAC data rule out that version of the $SU(2)_L \times SU(2)_R \times U(1)$ model which predicted no parity-violation (to lowest order); however, other versions of that model reproduce the WS model's predictions for all neutral-current phenomena.

IV. CONCLUSIONS

The discussion in Sections II and III indicated that most models are ruled out by present analyses, but that the WS model and certain corresponding $SU(2) \times U(1) \times G$ models survive. In general, those models which fail are ruled out by many standard deviations. In contrast, the $SU(2) \times U(1)$ model of Weinberg and Salam agrees within 90% confidence levels with 17 different experimental numbers as shown in the Table. Note that at the 90% confidence level one would expect about 2 of the 17 numbers to disagree with the theory; the fact that none disagrees may indicate that the error bars are conservative. Clearly one should not use only one standard deviation since then 6 numbers would be expected to disagree with theory. Left out of the Table are the results from the atomic parity-violation experiments since there are conflicting experimental results.

If one chooses to believe both the Oxford-Washington result and the SLAC result (and assuming there is no large y dependence), then the standard WS model fails. However, there is a simple extension[28] of the model which can account for all of these phenomena. Consider the group $SU(2) \times U(1) \times U(1)_R$ where neutrinos are neutral under $U(1)_R$. Then all

TABLE

Comparison of WS Theory with Experiment. The theoretical numbers for exclusive pion production contain 30% errors as discussed in the text.

Process	Quantity Measured	90% Confidence Experimental Limits (Statistical + Systematics)	WS Theory $\sin^2\theta_W = 0.25$
$\nu N \to \nu X$	R	.295 ± .02	.31
$\bar{\nu} N \to \bar{\nu} X$	R	.34 ± .05	.36
$\nu N \to \nu \pi X$	N_{π^+}/N_{π^-}	.77 ± .22	.82
$\bar{\nu} N \to \bar{\nu} \pi X$	N_{π^+}/N_{π^-}	1.64 ± .58	1.18
$\nu p \to \nu p$	R	.11 ± .05	.11
$\bar{\nu} p \to \bar{\nu} p$	R	.19 ± .10	.12
$\nu p \to \nu p \pi^0$	R	.56 ± .16	.42 ± .13
$\nu n \to \nu n \pi^0$	R	.34 ± .15	.43 ± .13
$\nu n \to \nu p \pi^-$	R	.45 ± .20	.28 ± .08
$\nu p \to \nu n \pi^+$	R	.34 ± .12	.28 ± .08
$\bar{\nu} N \to \bar{\nu} N \pi^0$	R	.57 ± .16	.39 ± .12
$\bar{\nu} n \to \bar{\nu} p \pi^-$	R	.58 ± .26	.29 ± .09
$\nu_\mu e \to \nu_\mu e$	$\frac{\sigma}{E}\left(\frac{cm^2}{GeV}\right)$	$(1.5 \pm 1.5) \times 10^{-42}$	1.4×10^{-42}
$\bar{\nu}_\mu e \to \bar{\nu}_\mu e$	$\frac{\sigma}{E}\left(\frac{cm^2}{GeV}\right)$	$(1.9 \pm 1.8) \times 10^{-42}$	1.4×10^{-42}
$\bar{\nu}_e e \to \bar{\nu}_e e (1.5 < E_e < 3.0)$	σ (cm^2)	$(5.96 \pm 2.7) \times 10^{-43}$	5.94×10^{-43}
$\bar{\nu}_e e \to \bar{\nu}_e e (3.0 < E_e < 4.5)$	σ (cm^2)	$(3.21 \pm 1.3) \times 10^{-43}$	2.53×10^{-43}
$e_{pol}\ D \to e\ X$	A/Q^2	(9.5 ± 2.[illegible]) $\times 10^{-5}$	7.2×10^{-5}

charged-current interactions and all neutrino interactions are unaffected. The parity-violation experiments here reflect the current

$$J_\mu^{WS} + \rho\, J_\mu^{I=0} \tag{4.1}$$

where the current resulting from $U(1)_R$ is isoscalar ($\bar{u}u + \bar{d}d$), and ρ is a free parameter which is taken to be small (say 0.1 or 0.2). Since the SLAC result involves differences between u_L and d_L (u_R and d_R), it is little affected by an isoscalar piece (which is multiplied by a small number). However, in the bismuth experiment one measures sums of u_L and d_L, and one finds that it is possible to cancel the effect due to the WS current. While it is possible to achieve this cancellation, it might seem to be a rather artificial or "unnatural" solution to this problem—obtaining zero by cancelling two large numbers against each other.

For the time, it might be best to wait for further atomic physics results on bismuth, thallium and hydrogen before reaching final conclusions. Nonetheless, the essential nature of the weak neutral-current interactions has become quite clear and the success of the Weinberg-Salam model is evident.

ACKNOWLEDGMENTS

The work described here was completed with Larry Abbott. I have benefited from discussions with S. Adler, J. Bjorken, F. Gilman, B. Kayser, W. Kozanecki, W. Marciano, J. Marriner, C. Matteuzzi, E. Monsay, F. Nezrick, Y.-J. Ng, E. Paschos, B. Ros, D. Sidhu, J. Strait, L. Sulak, S. Weinberg, and T. C. Yang. I would like to thank the Aspen Center for Physics (where this talk was prepared) and the Brookhaven National Laboratory theory group (where the written version was prepared) for the stimulating atmosphere each provided and for their hospitality.

REFERENCES

1. L. F. Abbott and R. M. Barnett, Phys. Rev. Lett. 40, 1303 (1978) and SLAC-PUB-2136 (1978) (submitted to Physical Review D). There are many other general discussions of neutral currents; among them are: D. P. Sidhu and P. Langacker, report No. BNL-24393 (1978) and Phys. Lett. 74B, 233 (1978); E. A. Paschos, report No. BNL-24619 (1978) and Phys. Rev. D15, 1966 (1977); F. E. Paige et al., Phys. Rev. D15, 3416 (1977); B. Kayser, NSF report (1978), invited talk at Int. Conf. on Neutrino Physics and Neutrino Astrophysics, Lafayette, Ind., April 28 - May 2, 1978; J. J. Sakurai, report No. UCLA/78/TEP/18 (1978), invited talk at Topical Conf. on Neutrino Physics at Accelerators, Oxford, England, July 4-9, 1978; UCLA/78/TEP/9 (1978), presented at Current Trends in Theory of Fields - 50 years of the Dirac Equation, Tallahassee, Fla., April 6-7, 1978; UCLA/77/TEP/23 (1977), presented at Irvine Conf. on Leptons and Quarks, Irvine, CA, Dec. 2-3, 1977; UCLA/77/TEP/15 (1977), invited talk at Neutrino 77, Elbrus, USSR, June 18-24, 1977; UCLA/76/TEP/21 (1976), invited lectures at Int. School of Subnuclear Physics, Erice, Sicily, June 23 - Aug. 8, 1976; Phys. Rev. Lett. 35, 1037 (1976); in Proc. 4th Int. Conf. on Neutrino Physics and Astrophysics, Dowington, PA., Apr. 26-28, 1974; P. Q. Hung and J. J. Sakurai, Phys. Lett. 72B, 208 (1977), 69B, 323 (1977) and 63B, 295 (1976); G. Ecker, Phys. Lett. 72B, 450 (1978); R. E. Hendrick and L.-F. Li, Carnegie-Mellon report (June 1978); see also Ref. 5, 7 and 10.

2. S. Weinberg, Phys. Rev. Lett. 19, 1264 (1967); A. Salam, in Elementary Particle Physics: Relativistic Groups and Analyticity, edited by N. Svartholm (Almquist and Wiksell, Stockholm, 1968), p. 367.

3. S. L. Glashow, J. Iliopoulos and L. Maiani, Phys. Rev. D2, 1285 (1970).

4. M. Holder et al. (CDHS), Phys. Lett. 72B, 254 (1977); J. Blietschau et al. (Gargamelle), Nucl. Phys. B118, 218 (1977); A. Benvenuti et al. (HPWF), Phys. Rev. Lett. 37, 1039 (1976); P. Wanderer et al. (HPWF), Phys. Rev. D17, 1979 (1978); F. S. Merritt et al. (CF), Phys. Rev. D17, 2199 (1978); P. C. Bosetti et al. (BEBC), Phys. Lett. 76B, 505 (1978).

5. L. M. Sehgal, Phys. Lett. 71B, 99 (1977); P. Q. Hung, Phys. Lett. 69B, 216 (1977); P. Scharbach, Nucl. Phys. B82, 155 (1974); and Ref. 1; recent work: S. Sarkar, Pennsylvania preprint, July 1978.

6. H. Kluttig et al., Phys. Lett. 71B, 446 (1977); J. Marriner, report No. LBL-6438 (1977), Univ. of California Ph. D. Thesis; B. Roe, invited talk at the Topical Conf. on Neutrino Physics at Accelerators, Oxford, England, July 4-9, 1978.

7. Analyses of elastic scattering have been done by S. Weinberg, Phys. Rev. D5, 1412 (1972); M. Barnett, Phys. Rev. D14, 2990 (1976); C. H. Albright et al., Phys. Rev. D14, 1780 (1976); V. Barger and D. V. Nanopoulos, Nucl. Phys. B124, 426 (1977); D. P. Sidhu, Phys. Rev. D14, 2235 (1976); F. Martin, Nucl. Phys. B104, 111 (1976); J. J. Sakurai and L. F. Urrutia, Phys. Rev. D11, 159 (1975).

8. L. Sulak, Harvard report, to appear in the Proc. of the Neutrinos-78 Conf., Purdue University, April 28 - May 2, 1978; J. B. Strait and W. Kozanecki, Harvard University Ph. D. theses (1978); D. Cline et al., Phys. Rev. Lett. 37, 252 and 648 (1976); see also W. Lee et al., Phys. Rev. Lett. 37, 186 (1976); M. Pohl et al., Phys. Lett. 72B, 489 (1978).

9. W. Krenz et al., report No. CERN/EP/PHYS 77-50 (1977); O. Erriques et al., Phys. Lett. 73B, 350 (1978); see also S. J. Barish et al., Phys. Rev. Lett. 33, 448 (1974); W. Lee et al., Phys. Rev. Lett. 38, 202 (1977).

10. S. L. Adler, Ann. Phys. 40, 189 (1968), and Phys. Rev. D12, 2644 (1975); S. L. Adler et al., Phys. Rev. D12, 3501 (1975) and Phys. Rev. D13, 1216 (1976); see also E. H. Monsay, Argonne report ANL-HEP-PR-78-08 (1978); G. Ecker in Ref. 7; and Ref. 1.

11. R. M. Barnett, Phys. Rev. Lett. 34, 41 (1975), Phys. Rev. D11, 3246 (1975); P. Fayet, Nucl. Phys. B78, 14 (1974); F. Gürsey and P. Sikivie, Phys. Rev. Lett. 36, 775 (1976); P. Ramond, Nucl. Phys. B110, 214 (1976).

12. R. M. Barnett, Phys. Rev. D13, 671 (1976).

13. A. De Rújula et al., Phys. Rev. D12, 3589 (1976); F. A. Wilczek et al., Phys. Rev. D12, 2768 (1975); H. Fritzsch et al., Phys. Lett. 59B, 256 (1975); S. Pakvasa et al., Phys. Rev. Lett. 35, 702 (1975).

14. R. M. Barnett, Phys. Rev. D15, 675 (1977).

15. B. W. Lee and S. Weinberg, Phys. Rev. Lett. 38, 1237 (1977); B. W. Lee and R. E. Shrock, Phys. Rev. D17, 2410 (1978); C. Segre and J. Weyers, Phys. Lett. 65B, 243 (1976).

16. R. M. Barnett and L. N. Chang, Phys. Lett. 72B, 233 (1977); R. M. Barnett et al., Phys. Rev. D17, 2266 (1978); P. Langacker and G. Segre, Phys. Rev. Lett. 39, 259 (1977).

17. J. Pati and A. Salam, Phys. Rev. D10, 275 (1974); H. Fritzsch and P. Minkowski, Nucl. Phys. B103, 61 (1976); R. N. Mohapatra and D. P. Sidhu, Phys. Rev. Lett. 38, 667 (1977); A. De Rújula, H. Georgi and S. L. Glashow, Ann. Phys. 109, 242 and 258 (1977).

18. H. Georgi and S. Weinberg, Phys. Rev. D17, 275 (1978); R. Gatto and F. Strocchi, Geneva report (1978).

19. P. E. G. Baird et al., Nature 264, 528 (1976).

20. N. Fortson, to appear in the Proc. of the Neutrinos-78 Conf., Purdue University, April 28 - May 2, 1978; E. Henley ibid.; W. J. Marciano and A. I. Sanda, Phys. Rev. D17, 3055 (1978) and Rockefeller report No. COO-2232B-153 (1978); G. Feinberg, Columbia report No. CU-TP-111, to appear in the Proc. of the Ben Lee Memorial Int. Conf., Batavia, Ill., Oct. 20-22, 1977.

21. P. G. H. Sandars, in Proc. 1977 Int. Symp. on Lepton and Photon Interactions at High Energies, edited by F. Gutbrod (DESY, Hamburg, 1977) p. 599.

22. L. M. Barkov and M. S. Zolotorev, Pisma Zh. Eksp. Teor. Fiz. (JETP Lett) 26, 379 (1978).

23. F. J. Hasert et al., Phys. Lett. 46B, 121 (1973); J. Blietschau et al., Nucl. Phys. B114, 189 (1976); H. Faissner et al., Phys. Rev. Lett. 41, 213 (1978); A. M. Cnops et al., Phys. Rev. Lett. 41, 357 (1978); P. Alibran et al., Phys. Lett. 74B, 422 (1978); F. Reines et al., Phys. Rev. Lett. 37, 315 (1976).

24. C. Y. Prescott et al., report No. SLAC-PUB-2148 (1978).

25. R. N. Cahn and F. J. Gilman, Phys. Rev. D17, 1313 (1978) and references therein.

26. J. D. Bjorken, report No. SLAC-PUB-2146 (1978).

27. W. J. Marciano and A. I. Sanda, Rockefeller report No. COO-2232B-142 (1978).

28. Private communications from J. D. Bjorken and T. C. Yang. It is possible that other people have also considered such an extension and its application to these two experiments.

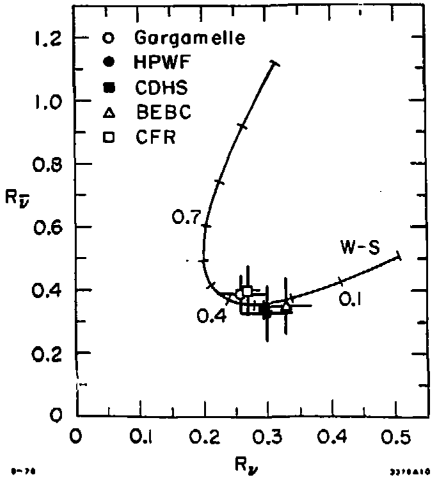

Fig. 1. The ratio of neutral to charged-current deep-inelastic scattering cross sections for antineutrinos versus that ratio for neutrinos. The curve shows the predictions of the WS model as a function of $\sin^2\theta_W$ (each tick mark indicates a tenth value of $\sin^2\theta_W$). The data are from Ref. 4.

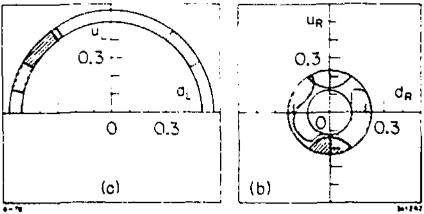

Fig. 2. The left (a) and right (b) coupling-constant planes. The lower half of (a) is omitted due to our sign convention $u_L \geq 0$. The annular regions are allowed by deep-inelastic data. The regions shaded with dots are allowed by inclusive-pion results, and the region shaded with lines is allowed by elastic and exclusive-pion data. Unique determination of the quark coupling values is given by the region shaded with both dots and lines.

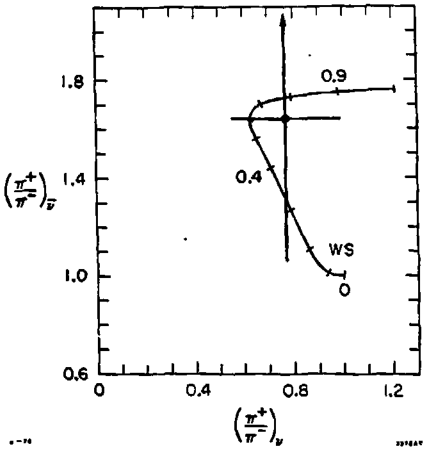

Fig. 3. The ratio of π^+ to π^- multiplicities from inclusive-pion data for antineutrinos versus that ratio for neutrinos. The curve shows the predictions of the Weinberg-Salam model as a function of $\sin^2\theta_W$. The data are from Ref. 5, and 90% confidence limits are shown.

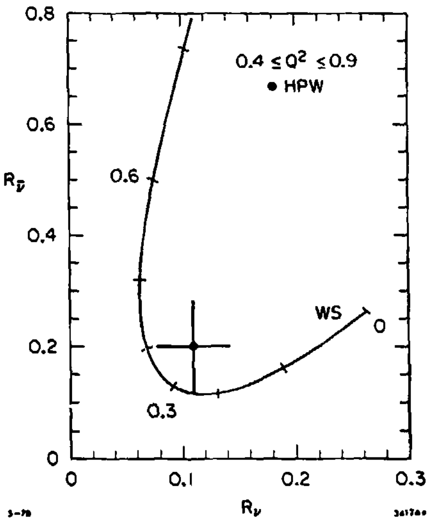

3-78
341744

Fig. 4. The ratio of neutral to charged-current elastic νp scattering cross sections for antineutrinos versus that ratio for neutrinos where $0.4 \leq Q^2 \leq 0.9$ GeV^2. The curve shows the predictions of the Weinberg-Salam model as a function of $\sin^2\theta_W$. The data are from Ref. 8, and only statistical uncertainties are shown (at the 90% confidence level).

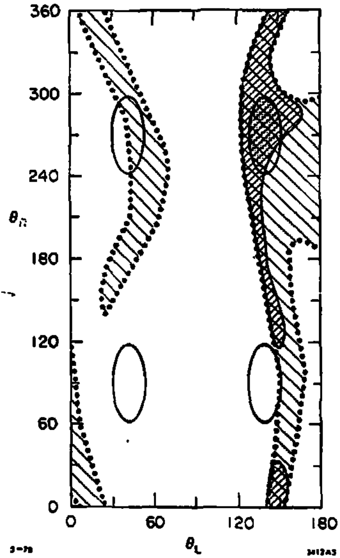

Fig. 5. The allowed angles in the coupling planes of Fig. 2 for fixed radii taken at the center of the allowed annulus (r_L = 0.53) in the left-coupling plane and at the outer edge of the allowed annulus (r_R = 0.22) in the right-coupling plane. The ellipses indicate the regions allowed by inclusive-pion data; going clockwise from the upper-right, they are regions A, B, C and D, respectively. The area shaded with lines and enclosed with a dotted curve is allowed by elastic data. The region which is cross-hatched is allowed by elastic and exclusive-pion results. The area shaded with dots is the only region allowed by all data.

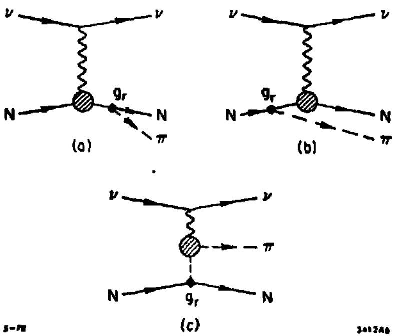

Fig. 6. Born diagrams for the exclusive-pion-production analysis. g_r is the pion-nucleon coupling constant.

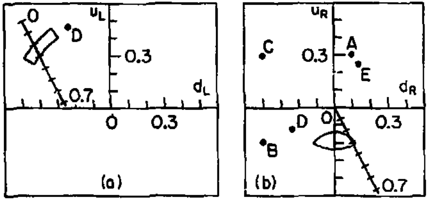

Fig. 7. Various gauge models compared with the allowed coupling-constant region. The lines mark the Weinberg-Salam model for values of $\sin^2\theta_W$ from 0.0 to 0.7. The points labeled A-E are the predictions of various models discussed in the text. For A, B, C, and E, u_L and d_L lie within the allowed region in the left-coupling plane.

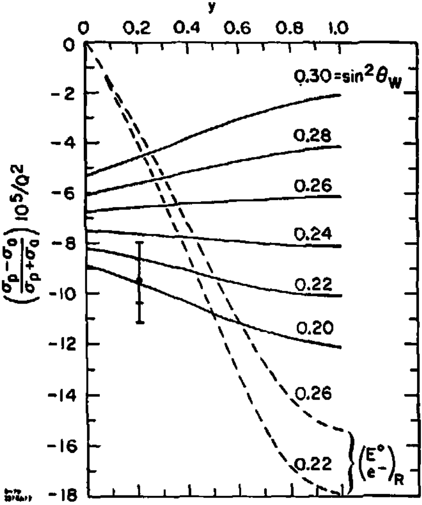

Fig. 8. The asymmetry in the SLAC experiment in which polarized electrons are inelastically scattered off deuterons, shown as a function of $y \equiv (E_e - E_e')/E_e$. The solid (dashed) curves are the predictions of the WS ("hybrid") model for various values of $\sin^2\theta_W$. The data are from Ref. 24 and have $Q^2 = 1.6\ \mathrm{GeV}^2$ and $y = 0.21$. σ_p and σ_a refer to cross sections for electrons polarized parallel and antiparallel to the beam.

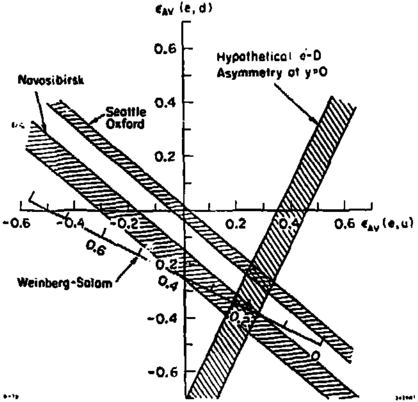

Fig. 9. Allowed values of $\epsilon_{AV}^{e,q}$, assuming that the measured deep-inelastic polarized-electron deuteron scattering asymmetry represents its value at y = 0.

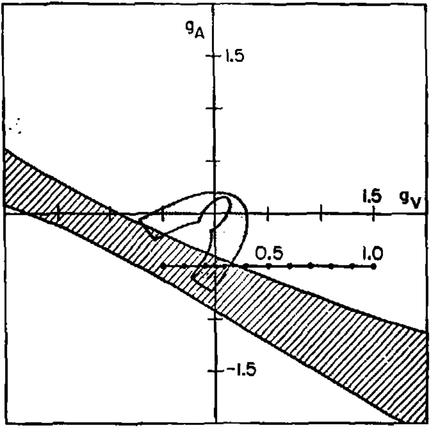

Fig. 10. Ninety percent confidence limits on g_A and g_V of the electron. The horseshoe-shaped area at the center of the figure is the overlap region allowed by the three types of νe scattering experiments. The band shaded with lines is the allowed region from the SLAC polarized-electron-deuteron scattering experiment (Ref. 24) assuming a single Z^0 boson and values from Sec. II of quark couplings (including quark error bars). The upper (lower) band shaded with dots is for the Washington-Oxford (Novosibirsk) parity-violation experiments. The predictions of the WS model are shown for tenth values of $\sin^2\theta_W$.